2- and 3-Substituted 1,4-Naphthoquinone Derivatives as Subversive Substrates of Trypanothione Reductase and Lipoamide Dehydrogenase from *Trypanosoma cruzi*: Synthesis and Correlation between Redox Cycling Activities and in Vitro Cytotoxicity

Laurence Salmon-Chemin,[†] Eric Buisine,[†] Vanessa Yardley,[‡] Sven Kohler,[§] Marie-Ange Debreu,[†] Valérie Landry,[†] Christian Sergheraert,[†] Simon L. Croft,[‡] R. Luise Krauth-Siegel,*,[§] and Elisabeth Davioud-Charvet*,[†]

UMR 8525 CNRS - Université Lille II, Institut de Biologie de Lille et Institut Pasteur de Lille, 1 rue du Professeur Calmette, BP447, 59021 Lille Cedex, France, Department of Infections and Tropical Diseases, London School of Hygiene & Tropical Medicine, Keppel Street, London WC1E 7HT, U.K., and Biochemie-Zentrum der Universität Heidelberg, Im Neuenheimer Feld 328, D-69120 Heidelberg, Germany

Trypanothione reductase (TR) is both a valid and an attractive target for the design of new trypanocidal drugs. Starting from menadione, plumbagin, and juglone, three distinct series of 1,4-naphthoquinones (NQ) were synthesized as potential inhibitors of TR from *Trypanosoma cruzi* (TcTR). The three parent molecules were functionalized at carbons 2 and/or 3 by various polyamine chains. Optimization of TcTR inhibition and TcTR specificity versus human disulfide reductases was achieved with the 3,3′-[polyaminobis(carbonylalkyl)]bis(1,4-NQ) series **19–20**, in which an optimum chain length was determined for inhibition of the trypanothione disulfide reduction. The most active derivatives against trypanosomes in cultures were also studied as subversive substrates of TcTR and lipoamide dehydrogenase (TcLipDH). The activities were measured by following NAD(P)H oxidation as well as coupling the reactions to the reduction of cytochrome *c* which permits the detection of one-electron transfer. For TcTR, **20₄₋c** proved to be a potent subversive substrate and an effective uncompetitive inhibitor versus trypanothione disulfide and NADPH. Molecular modeling studies based on the known X-ray structures of TcTR and hGR were conducted in order to compare the structural features, dimensions, and accessibility of the cavity at the dimer interface of TcTR with that of hGR, as one of the putative NQ binding sites. TcLipDH reduced the plumbagin derivatives by an order of magnitude faster than the corresponding menadione derivatives. Such differences were not observed with the pig heart enzyme. The most efficient and specific subversive substrates of TcTR and TcLipDH exhibited potent antitrypanosomal activity in in vitro *T. brucei* and *T. cruzi* cultures. The results obtained here confirm that reduction of NQs by parasitic flavoenzymes is a promising strategy for the development of new trypanocidal drugs.

Introduction

The quinone structure is common to numerous natural products and is associated with anticancer, antibacterial, antimalarial, and fungicide activities.[1] In most cases, the biological activity is related to the ability of quinones to accept one and/or two electrons to form the corresponding radical anion or dianion species as well as the acid–base properties of the compounds. The cytoxicity of quinones is also often attributed to DNA modification, thiol and amine depletion by alkylation, oxidation of essential protein thiols by activated oxygen species, and/or glutathione disulfide (GSSG).[1] The variable capacity of quinones to accept electrons is due to the electron-attracting or -donating substituents at the quinone moiety[2] which modulate the redox properties

responsible for the resulting oxidative stress. The molecular basis of quinone toxicity is the enzyme-catalyzed reduction to semiquinone radicals which then reduce oxygen to superoxide anion radicals thereby regenerating the quinone.[1] This futile redox cycling and oxygen activation lead to increased levels of hydrogen peroxide and GSSG. A well-studied example is menadione (2-methyl-1,4-naphthoquinone), which is an acceptor of electrons from numerous flavoproteins acting through a one-electron mechanism, e.g. NADPH cytochrome *c* reductase, NADH dehydrogenase, and ferredoxin NADP reductase, or through a mixed mechanism (one- and two-electron), e.g. NAD(P)H dehydrogenase (or DT-diaphorase) or lipoamide dehydrogenase (LipDH).[3,4]

Many naphthoquinone (NQ) drugs, such as menadione, plumbagin, and lapachol, display notable trypanocidal activities upon different trypanosomes and *Leishmania* responsible for several human diseases including African sleeping sickness (*Trypanosoma brucei rhodesiense* and *Trypanosoma brucei gambiense*), Chagas' disease (*Trypanosoma cruzi*), and Kala-azar (*Leishmania donovani*).[5–7] These parasitic protozoa of the order
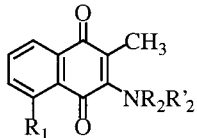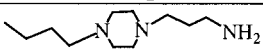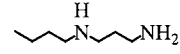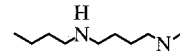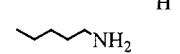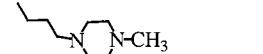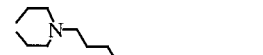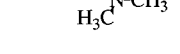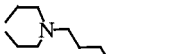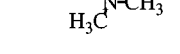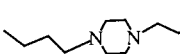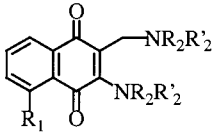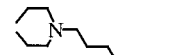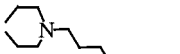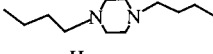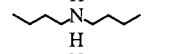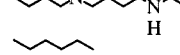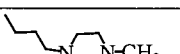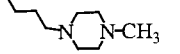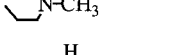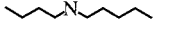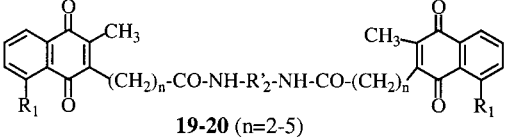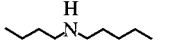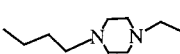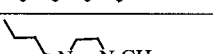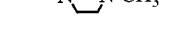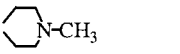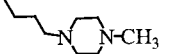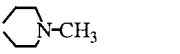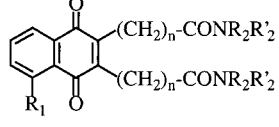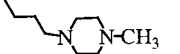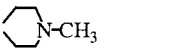
* To whom correspondence should be addressed. For E.D.-C.: Phone: (33) 3 20 87 12 17. Fax: (33) 3 20 87 12 33. E-mail: elisabeth.davioud@pasteur-lille.fr. For R.L.K.-S.: Phone: (49) 6221 54 41 87. Fax: (49) 6221 54 55 86. E-mail: krauth-siegel@urz.uni-heidelberg.de.
† UMR 8525 CNRS - Université Lille II.
‡ London School of Hygiene & Tropical Medicine.
§ Biochemie-Zentrum der Universität Heidelberg.

Chart 1. Structures of the Series of 1,4-NQs: 3-Polyamino-1,4-NQs **3–6**, 3-(Polyaminocarbonylalkyl)-1,4-NQs **16–17**, 2,3-Bis(polyaminocarbonylalkyl)-1,4-NQ **18**, and 3,3′-[Polyaminobis(carbonylalkyl)]bis(1,4-NQ)s **19–20**

Structure	NQ	R_1	R_2	R'_2
3-4	3_b	H	H	[piperazinyl–propyl–NH_2 chain]
	4_b	OH		
	3_c	H	H	[CH_3–N(H)–ethyl–NH_2 chain]
	4_c	OH		
	3_d	H	H	[propyl–N(H)–propyl–N(H)–ethyl–NH_2 chain]
	4_d	OH		
	3_e	H	H	[butyl–NH_2]
	4_e	OH		
	3_f	H	H	[4-methylpiperazinyl–ethyl chain]
	4_f	OH		
5	3_h	H	–	[piperidinyl–propyl–N(CH_3) chain, H_3C]
	5_h	H	–	[piperidinyl–propyl–N(CH_3) chain, H_3C]
6	6_b	H	–	[butyl–piperazinyl–butyl chain]
	6_c	H	–	[propyl–N(H)–propyl chain]
	6_d	H	–	[propyl–N(H)–propyl–N(H)–propyl chain]
	6_e	H	–	[pentyl chain]
16-17 (n=2-3)	$16_{n\text{-}f}$	H	H	[4-methylpiperazinyl–CH_3 chain]
	$17_{n\text{-}f}$	OH	H	
	$16_{n\text{-}g}$	H	–	[N-methylpiperidinyl, $N\text{-}CH_3$]
	$17_{n\text{-}g}$	OH	–	
19-20 (n=2-5)	$19_{n\text{-}a}$	H	–	[butyl–N(H)–butyl chain]
	$20_{n\text{-}a}$	OH	–	
	$19_{n\text{-}b}$	H	–	[butyl–piperazinyl–butyl chain]
	$20_{n\text{-}b}$	OH	–	
	$19_{n\text{-}c}$	H	–	[butyl–N(H)–propyl chain]
	$20_{n\text{-}c}$	OH	–	
18 (n=2-5)	$18_{n\text{-}f}$	OH	H	[4-methylpiperazinyl–CH_3 chain]
		OH	H	
	$18_{n\text{-}g}$	OH	–	[N-methylpiperidinyl, $N\text{-}CH_3$]
		OH	–	

Kinetoplastida are particularly sensitive to oxidative stress and have developed specific antioxidant systems.[8] In contrast to nearly all other organisms, they lack glutathione reductase (GR) but have a trypanothione reductase (TR) instead. The physiological substrate of TR is the bis-glutathionyl spermidine disulfide (trypanothione disulfide, T(S)$_2$), which is reduced to the corresponding dithiol trypanothione (T(SH)$_2$). Many ammonium compounds possessing substituted side chains have been described as effective and specific TR inhibitors. The selectivity of inhibitors for parasite TR over human GR (hGR) was mainly due to the charge differences at the catalytic sites of the two enzymes.[9] LipDH is another flavoenzyme, structurally and mechanisti-

cally closely related to TR and GR, and all belong to the family of FAD-disulfide oxidoreductases.[10] A well-known function of LipDH is the NAD$^+$-dependent oxidation of protein-bound dihydrolipoamide in mitochondrial 2-oxoacid dehydrogenase complexes. TR and LipDH have been purified[11,12] from *Trypanosoma cruzi* (TcTR and TcLipDH), and the genes have been cloned and overexpressed.[13,14] Besides their physiological reactions, TR, GR, and LipDH catalyze the slow NAD(P)H-dependent reduction of molecular oxygen.[15] In the case of TcLipDH this intrinsic NADH oxidase activity amounts to about 1% of the physiological activity of the enzyme.[15,16] All three flavoenzymes have been shown to interact with NQs. In the case of TcTR, menadione,

Chart 2. Structures of the Polyamines **a**−**h**

Scheme 1. Synthesis of 3-Polyamino-1,4-NQs **3**−**6**[a]

[a] Reaction conditions: (a) $R_2R'_2NH$ (5 equiv), EtOH−DCM; (b) $NH_2R'_2NH_2$ (0.5 equiv), EtOH−DCM.
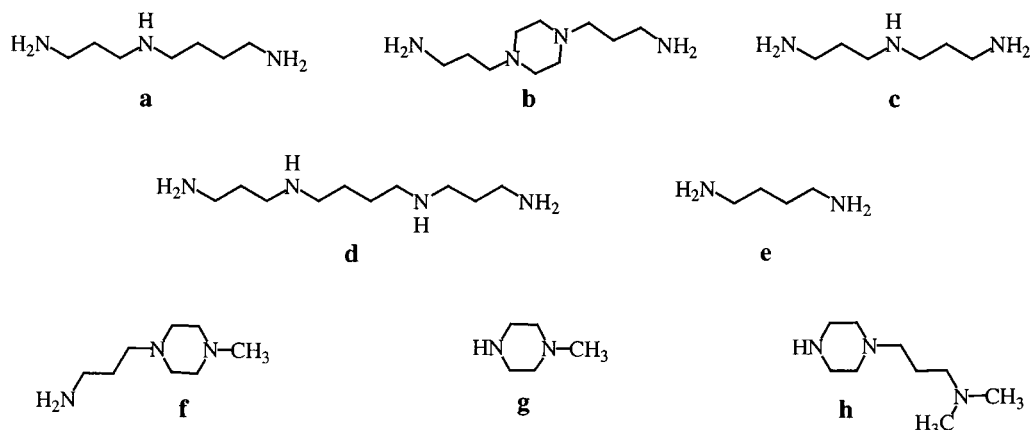
plumbagin,[17] and other 1,4-NQs[18−20] act as subversive substrates (or turncoat inhibitors) by inhibiting the physiological reduction of $T(S)_2$ and promoting a non-physiological reaction. In the presence of O_2, the one-electron reduction of quinones can lead to the production of superoxide anion radicals. Toward GR, 1,4-NQs act mainly as weak reversible inhibitors.[19,21,22] Since the three parent NQs are known to interact unspecifically with numerous NAD(P)H-dependent disulfide oxidoreductases, like TR,[17] GR,[23] LipDH,[4] and thioredoxin reductase[24] (TrxR), the aim of this work was to improve the specificity of NQs for TR binding and to decrease cytotoxicity against human cells.

In the present paper, we describe the synthesis of a series of menadione, plumbagin, and juglone derivatives, their inhibition potencies of TcTR, and their in vitro trypanocidal effects. The approach included the synthesis of cationic ligands displaying different redox potentials. For this purpose, the three parent structures were substituted at C-2 and C-3 of the quinone moiety (Chart 1) by alkylamino side chains of varying length (Chart 2), either attached directly or with an alkyl spacer of variable length via a bridging amide bond. Enzymatic and antitrypanosomal studies revealed that several NQ derivatives with strong trypanocidal activity were among the most effective TcTR inhibitors. However, the lack of correlation between inhibition of $T(S)_2$ reduction and antitrypanosomal action for several other NQs suggested a study of the redox cycling properties of the compounds toward TcTR and TcLipDH. These studies revealed that the most potent trypanocidal NQs displayed the highest and most specific redox cycling activities toward TcTR or TcLipDH. In addition, molecular modeling studies based on the known X-ray structures of TcTR and hGR[25−29] were conducted to obtain a deeper insight in the structural features, dimensions, and accessibility of the cavity at the dimer interface of TcTR and hGR, as one of the putative NQ binding sites.

Results

Synthesis of 3-Polyamino-1,4-NQ. A first series of 3-polyamino-1,4-NQ derivatives **3**−**6** was synthesized by direct 1,4-type addition of the quinone moiety of 1,4-NQ to polyamines **b**−**h** (Scheme 1). The nonisolated amino-substituted naphthohydroquinone intermediates were spontaneously oxidized by molecular oxygen, to allow the regeneration of the quinone moiety in the final products **3**−**6**.[30,31] The ethanol−DCM (2:0.5) mixture was found to be the solvent of choice for the reaction since it favored the solubility of both starting NQs and formed products. Attempts to improve the yields of the 3-polyaminoplumbagin derivatives **4** by changing the reaction conditions (solvent, temperature) proved unsuccessful. In comparison with EtOH alone or EtOH−DCM, DCM, or DMF as sole solvent led to the formation of many byproducts. Toluene was employed as a replacement for EtOH, but its handling proved difficult under reduced pressure leading to NQ degradation. Product mixtures were not less complex when the reaction temperature was reduced from 25 to 4 °C. In addition, product isolation and purification proved to be difficult in the case of aliphatic tri- or tetraamines. All compounds required purification by preparative TLC with an appropriate elution solvent (acetone/NH_4OH for mono derivatives and toluene/THF/TEA for bis derivatives). In the case of the secondary amine **h**, in addition to the expected product **3h**, the minor compound **5h** was isolated. This was the result of an addition−elimination reaction occurring during which the methyl group behaves as an electron donor to oxygen.[32] Nucleophilic substitution of bromo intermediates was also considered.[33] Three derivatives 3-bromo-2-methyl-1,4-NQ, 2-bromomethyl-1,4-NQ, and 3-bromo-2-bromomethyl-1,4-NQ were prepared by the bromination of menadione.[31] With the first two bromo derivatives, addition−elimination

Scheme 2. Synthesis of Carboxylic Acids **9−11** and Boc-Protected Amines **14−15**[a]

1 R_1 = H, R_3 = CH_3
2 R_1 = OH, R_3 = CH_3
7 R_1 = OH, R_3 = H

8₂ n = 2
8₃ n = 3
8₄ n = 4
8₅ n = 5

9₂₋₅ R_1 = H, R_3 = CH_3
10₂₋₅ R_1 = OH, R_3 = CH_3
11₂₋₅ R_1 = H, R_3 = -$(CH_2)_n$-COOH

12₂ n = 2
12₃ n = 3
12₄ n = 4
12₅ n = 5

13₂ n = 2
13₃ n = 3
13₄ n = 4
13₅ n = 5

1 R_1 = H
2 R_1 = OH

13₂ n = 2
13₃ n = 3
13₄ n = 4
13₅ n = 5

14₂₋₅ R_1 = H
15₂₋₅ R_1 = OH
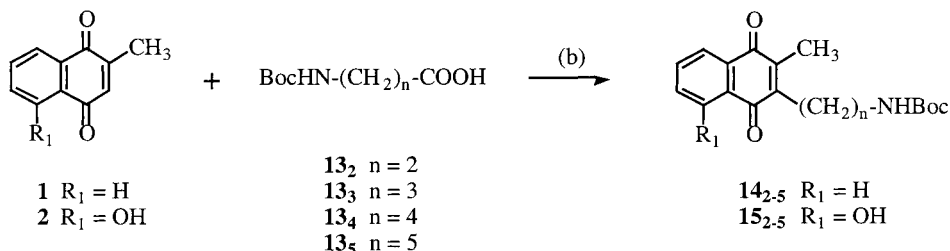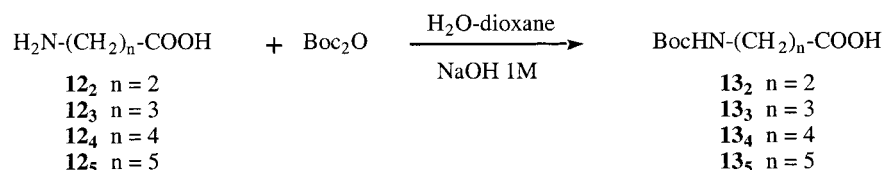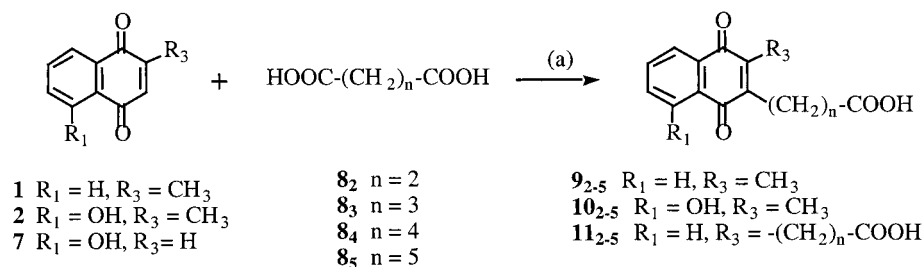
[a] Reaction conditions: (a) **9−10**: diacid (3 equiv), AgNO₃ catalytic, (NH₄)₂S₂O₈ (1.3 equiv), aq 30% CH₃CN, 60−65 °C; **11**: diacid (6 equiv), AgNO₃ catalytic, (NH₄)₂S₂O₈ (2.6 equiv), aq 30% CH₃CN, 60−65 °C; (b) **14−15**: Boc-protected amines **13₂₋₅** (3 equiv), AgNO₃ catalytic, (NH₄)₂S₂O₈ (1.3 equiv), aq 30% CH₃CN, 60−65 °C.

Scheme 3. Synthesis of Amides **16−18** and Bis(amides) **19−20**[a]

9₂₋₅ R_1 = H, R_3 = CH_3
10₂₋₅ R_1 = OH, R_3 = CH_3
11₂₋₅ R_1 = OH, R_3 = -$(CH_2)_n$-COOH

16₂₋₃, f-g R_1 = H, R_3 = CH_3
17₂₋₃, f-g R_1 = OH, R_3 = CH_3
18₂₋₅, f-g R_1 = OH, R_3 = -$(CH_2)_n$-CONR₂R'₂

9₂₋₅ R_1 = H
10₂₋₅ R_1 = OH

19₂₋₅, a-c R_1 = H
20₂₋₅, a-c R_1 = OH
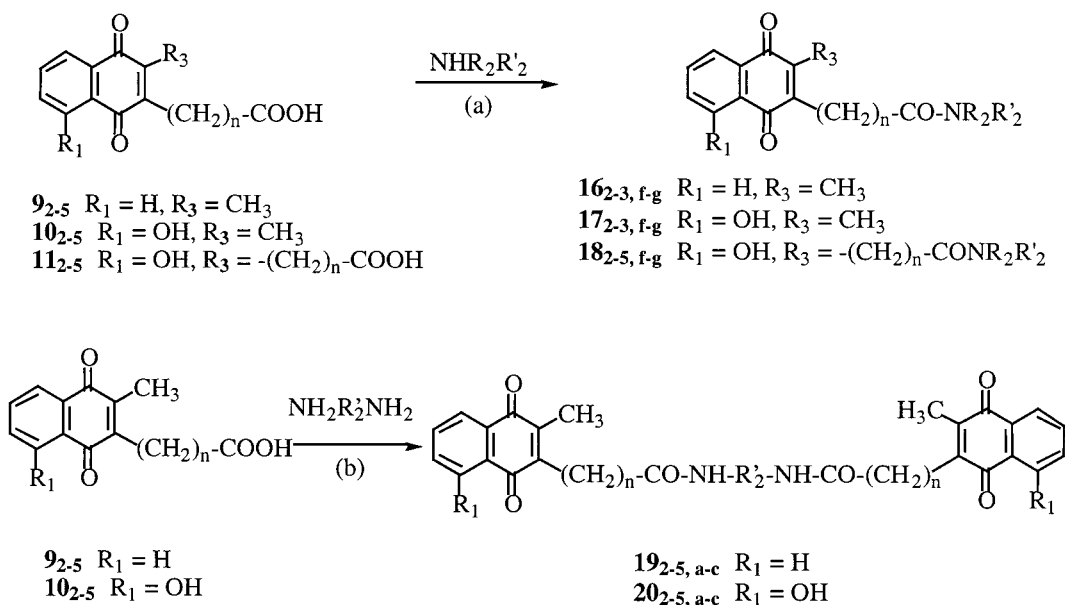
[a] Reaction conditions: (a) **16−17**: NHR₂R'₂ (1 equiv), HBTU (1 equiv), DIEA (3 equiv), DCM−DMF, rt, 3 h; **18**: NHR₂R'₂ (2 equiv), HBTU (2 equiv), DIEA (6 equiv), DCM−DMF, rt, 3 h; (b) NH₂R'₂NH₂ (0.5 equiv), HBTU (1 equiv), DIEA (1 equiv), DCM−DMF, rt, 3 h.

did not lead to the major products described by Ohta et al.[31] Only compound **5h** was obtained as the major product from the reaction of polyamine **h** and 3-bromo-2-bromomethyl-1,4-NQ.[34] However, in the plumbagin series, 1,4-type addition followed by oxidation in air led to low yields and many byproducts. Synthesis of 3,3′-polyaminobis(1,4-NQ) **6** was achieved by inverse addi-

tion of polyamine (1 equiv) to menadione as starting material (2 equiv).

Synthesis of 3-(Polyaminocarbonylalkyl)-1,4-NQ. Our aim was to synthesize in a high-yield two-step procedure a second series of 1,4-NQ possessing an amino side chain, with a nitrogen atom nonconjugated with the quinone portion of 1,4-NQ. Since 1,4-NQs are highly

Table 1. Inhibitory and Redox Cycling Activities toward TcTR and in Vitro Antiparasitic Activities of Compounds **3−6** and **16−18**

compd	n	series	IC$_{50}$^{a} (μM)	x-fold^b (100 μM)	ED$_{50}$ (μM) L. donovani^c	T. cruzi^c	T. brucei
3$_b$		menadione	6	×2.2	≥12.5*	≥12.5	>12.5
3$_c$		(R$_1$ = H)	12	nd	>12.5*	≥12.5	>12.5
3$_d$			28	nd	T/100^d	T/+^{g}	30
3$_e$			>57	nd	>12.5	T/+^{f}	>12.5
3$_f$			>57	×2	≥ 6.2*	≥ 6.2	>12.5
3$_h$			>57	nd	>12.5*	>12.5	>12.5
4$_b$		plumbagin	39	×6.4	T/+^{d}	T/+^{f}	>3
4$_c$		(R$_1$ = OH)	57	×2	>30	T/+^{g}	>12.5
4$_d$			28	nd	>30	T/+^{g}	>30
4$_e$			>57	nd	>6.2*	>12.5	>12.5
4$_f$			>57	×2.8	T/100^d	T/+^{e}	>12.5
5$_h$		menadione	>57	×3.9	>12.5*	>12.5	>12.5
6$_b$		(R$_1$ = H)	10	nd	T/+^{e,*}	T/+^{e}	>12.5
6$_c$			9	×4	≥ 12.5*	T/+^{e}	>12.5
6$_d$			6.5	nd	T/100^d	T/+^{g}	>1
6$_e$			>57	nd	>12.5*	>12.5	>12.5
16$_{2-f}$	2	menadione	38	×7	>30	T/+^{d}	>10
16$_{2-g}$		(R$_1$ = H)	>50	×19	87	70	9.5
17$_{2-f}$	2	plumbagin	16	×10	nd	T/+^{e}	>10
17$_{2-g}$		(R$_1$ = OH)	50	×38	>88	>88	52
16$_{3-f}$	3	menadione	44	×11	>76	>76	46
16$_{3-g}$		(R$_1$ = H)	nd	nd	32	27	9.1
17$_{3-f}$	3	plumbagin	32	×40	66	50	23
17$_{3-g}$		(R$_1$ = OH)	42	×14	82	>84	52
18$_{2-f}$	2	juglone	>50	nd	>50	>50	21.5
18$_{2-g}$			>50	nd	>62	>62	22.2
18$_{3-f}$	3		11	×45	>59	59	259
18$_{3-g}$			17.5	×220	>48	>48	31.4
18$_{4-f}$	4		6.2	nd	38.2	>46	>15
18$_{4-g}$			5.9	nd	T/100^f	T/+^{e}	>56
18$_{5-f}$	5		0.8	nd	T/+^{e}	T/+^{d}	10.1
18$_{5-g}$			2.9	nd	T/+^{f}	T/+^{f}	13.1

^{a} In the presence of 57 μM T(S)$_2$. ^{b} The redox cycling activities of compounds were measured at 25 °C in TR assay buffer, pH 7.25, at an NADPH concentration of 250 μM, as described in the Experimental Section. The control assays which contained only NADPH and the enzyme represent the intrinsic oxidase activity of TR. Oxidation of NADPH was monitored at 340 nm. The rate of NADPH oxidation by TcTR in the presence of 100 μM NQ was x-fold increased, when compared to the intrinsic oxidase activity of the enzyme (17-fold for menadione and 39-fold for plumbagin). nd, not determined. ^{c} T/100 means the compound was toxic to macrophages, 100% inhibition; T/+ means the compound was toxic to macrophages but parasites were still present: ^{d}at 30 μM, ^{e}at 10 μM, ^{f}at 3 μM, ^{g}at 1 μM. *L. infantum.

reactive, it was necessary to find a general route which allowed the preparation of intermediates under mild conditions, which could be easily derivatized by parallel synthesis. Both solid- and solution-phase methodologies allowing parallel syntheses of a large array of diverse amino-substituted NQs have recently been described.[35] Taking into account that many polyamines were commercially available, we selected a versatile reaction to prepare 1,4-NQ acid and amine derivatives as intermediates in the synthesis of a large array of amides by standard coupling procedures in solution. Diacids of varying length (succinic acid, glutaric acid, adipic acid, and pimelic acid) were reacted with menadione or plumbagin, via the oxidative decarboxylation of acids, promoted by silver salts as an efficient catalyst in the presence of ammonium peroxydisulfate[36] (Scheme 2). In this way, eight 1,4-NQ acid derivatives **9−10** were prepared in bulk. HBTU was used as coupling reagent, and the reaction was performed in solution (Scheme 3). The 3-(polyaminocarbonylalkyl)-1,4-NQs **16−17** and the 3,3′-[polyaminobis(carbonylalkyl)]bis(1,4-NQ)s **19−20** were prepared from polyamines **f−g** and from polyamines **a−c**, respectively, with the latter possessing two terminal amino groups.

Synthesis of 3-(*N*-Boc-aminoalkyl)-1,4-NQ. By the same method, *N*-Boc-protected 1,4-NQ amines **14**−**15** were synthesized from *N*-Boc-protected amino acids **13**, previously prepared from the corresponding amino acids **12**, β-alanine, γ-aminobutyric acid, 5-aminovaleric acid, and 6-aminocaproic acid (Scheme 2).

Synthesis of 2,3-Bis(polyaminocarbonylalkyl)-1,4-NQ. As described above for the synthesis of mena-dione and plumbagin acid derivatives, four juglone diacids **11** were synthesized from the four starting diacids (Scheme 2). Then, 2,3-bis(polyaminocarbonyla-lkyl)-1,4-NQs **18** were prepared by coupling in solution diacids **11** with polyamines **f**−**g** in the presence of HBTU as coupling reagent (Scheme 3). Noteworthy here is that the structures of the synthesized juglone deriva-tives resembled more closely the structures of the plumbagin derivatives than that of juglone itself. Ju-glone derivatives can therefore be classified as plum-bagin derivatives because of the presence of methylene groups at C-2 and C-3.

Inhibition of TR-Catalyzed T(S)₂ Reduction. The three series of 1,4-NQs **3**−**6**, **9**−**11**, and **14**−**20** were tested in the T(S)₂ reduction assay at varying concen-trations (0.3−50 μM), by following the disappearance of NADPH at 340 nm (Tables 1−3). For each NQ, we checked at the concentration corresponding to the IC₅₀ value that the rate of NADPH oxidation was negligible in the absence of T(S)₂, proving that the NQ used in the presence of a low amount of TcTR (0.02 U/assay) behaved as an inhibitor. When tested as potential inhibitors of the TR-catalyzed T(S)₂ reduction in the presence of 57 μM T(S)₂ and TR, the respective IC₅₀ values of the 3-polyamino-1,4-NQ derivatives **3b**, **3c**, **3d** and 3,3′-polyaminobis(1,4-NQ) derivatives **6b**, **6c**, **6d** were found to be lower than those of the parent molecule, menadione (IC₅₀ = 55 μM) (Table 1). In contrast compound **6e** lacking a protonatable nitrogen atom in the side chain was not well-recognized by TcTR, which illustrates the essential requirement of a posi-tively charged amino group for TR recognition. None of the plumbagin derivatives yielded an IC₅₀ value lower than that of plumbagin (IC₅₀ = 28 μM). Using the routine procedure, we also tested the 12 acid derivatives **9**−**11** at 50 μM and the 8 *N*-Boc-protected amine derivatives **14**−**15** at either 25 or 50 μM (Table 2). No inhibition of TcTR was observed. This was not so surprising with the acid derivatives **9**−**11** since similar results have already been reported with a variety of molecules bearing a carboxylic group,[9,37] proving once more the importance of the charge as the major dis-criminating factor for TR/GR specificity. Most of the 3-(polyaminocarbonylalkyl)-1,4-NQs **16**−**17** were rela-tively ineffective with little TcTR inhibition evident at concentrations up to 50 μM (16 < IC₅₀ < 50 μM) (Table 1). When compared with **g**, amine **f**, in agreement with the increased number of protonable amino groups of the side chain (2 instead of 1), conferred a greater inhibitory potency in the series of compounds **16**−**17**. However, the 2,3-polyaminocarbonylalkyl-1,4-NQ **18** (Table 1) and the 3,3′-[polyaminobis(carbonylalkyl)]bis(1,4-NQ)s **19**−**20** (Table 3) exhibited significant inhibition in the low-micromolar range (IC₅₀ < 5 μM), particularly when the length of the alkyl linker reached a maximum (*n* = 4 or 5 methylene groups). The bis(1,4-NQ) **20₄₋c** was found

Table 2. Inhibitory Activities toward TcTR and in Vitro Antiparasitic Activities of Carboxylic Acids **9**−**11** and Boc-Protected Amines **14**−**15**
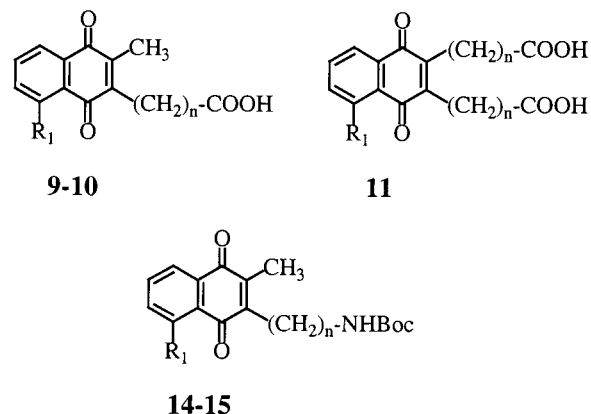
compd	*n*	series	IC₅₀[a] (μM)	ED₅₀ (μM) *L. donovani*	*T. cruzi*	*T. brucei*
9₂	2	menadione	>50	>30	>30	>30
9₃	3	(R₁ = H)	>50	>116	>116	75
9₄	4		>50	39	44	>110
9₅	5		>50	18	17	5.3
10₂	2	plumbagin	>50	72	46	>11
10₃	3	(R₁ = OH)	>50	>109	>109	78
10₄	4		>50	56	42	>10
10₅	5		>50	28	32	>3.3
11₂	2	juglone	>50	>93	>94	59
11₃	3		>50	>87	>87	61
11₄	4		>50	>80	80	>80
11₅	5		>50	>74	>74	48
14₂	2	menadione	>50	8.8	9.5	0.9
14₃	3	(R₁ = H)	>50	29.4	13.8	>3
14₄	4		>25	16.5	10.4	>3
14₅	5		>50	12.5	4.3	2.7
15₂	2	plumbagin	>25	11.8	3.5	0.6
15₃	3	(R₁ = OH)	>25	10.0	3.7	0.6
15₄	4		>25	14.2	7.0	1.4
15₅	5		>25	33.8	13.3	2.5

[a] In the presence of 57 μM T(S)₂. The assays were carried out as described in the legend of Table 1.

to be the most potent TcTR inhibitor with an IC₅₀ of 0.45 μM in the presence of 57 μM T(S)₂, a value 62-fold lower than the corresponding parent molecule, plum-bagin (IC₅₀ = 28 μM) (Table 3). To determine the inhibition type, TcTR activity was measured in the presence of varying concentrations of T(S)₂ (25−200 μM) and constant concentrations of the mono(NQ) **3b** (0−40 μM) and the bis(NQ) **20₄₋c** (0−2 μM), respectively. The type of inhibition was deduced from Lineweaver−Burk, Dixon, and Cornish−Bowden plots.[38] While inhibition of TcTR by **3b** was noncompetitive (data not shown), **20₄₋c** acted as an uncompetitive inhibitor toward T(S)₂ (Figure 1). An inhibition constant of 0.5 ± 0.02 μM was calculated by fitting the data to the appropriate equa-tion by a computerized least-squares regression.[38] With NADPH (5−25 μM) as variable substrate and T(S)₂ at a constant concentration of 100 μM, inhibition of TR by **20₄₋c** (0−2.5 μM) was also uncompetitive.

TcTR versus hGR and hTrxR Specificity Stud-ies. The most potent TR inhibitor **20₄₋c** was also measured as inhibitor of hGR. In the presence of 50 μM GSSG, the IC₅₀ value was 10 μM which is 22-fold higher than the value for TR. The corresponding IC₅₀ values of the parent molecules were quite similar for the

Table 3. Inhibitory, Redox Cycling, and in Vitro Antiparasitic Activities of Compounds **19−20** toward TcTR

compd	n	series	IC$_{50}$[a] (μM)	x-fold[b] (25 μM)	K_m (μM)	V_{max} (μmol/min/mg)	k_{cat}/K_m (10^4 M^{-1} s^{-1})	ED$_{50}$ (μM) *L. donovani*[c]	*T. cruzi*[c]	*T. brucei*
menadione			55	×15	21	0.26	1.0	T/100[d]	T/100[e]	inactive[d]
plumbagin			28	×21	15	0.31	1.7	T/100[f]	T/100[e]	1.5
19$_{2-a}$	2	menadione	2.7	×117	30	1.83	5.1	>50	13	4.9
19$_{2-b}$		(R$_1$ = H)	3.7	×40[#]	14	0.74	4.4	>46	40	3.2
19$_{2-c}$			5	×69	47	1.30	2.3	>51	47	4.5
20$_{2-a}$	2	plumbagin	2.9	×199	48	4.44	7.7	>48	46	13.8
20$_{2-b}$		(R$_1$ = OH)	2.6	×158	78	4.74	5.1	>44	44	30.3
20$_{2-c}$			1.9	×154	230	12.43	4.5	>49	13	1.7
19$_{3-a}$	3	menadione	4.0	×62	74	2.04	2.3	>48	>48	26.6
19$_{3-b}$		(R$_1$ = H)	4.5	×50	12	0.6	4.2	14.7	13	13.7
19$_{3-c}$			11	×25	23	0.45	1.6	>49	>49	27.0
20$_{3-a}$	3	plumbagin	2.3	×100	93	4.0	3.6	>46	46	>4.5
20$_{3-b}$		(R$_1$ = OH)	2.3	×83	52	2.16	3.5	38.5	28	3.4
20$_{3-c}$			2.0	×165	55	4.29	6.5	46.7	47	>4.6
19$_{4-a}$	4	menadione	1.4	×76	16	1.11	5.8	11.9	9	4.4
19$_{4-b}$		(R$_1$ = H)	1.1	×117	16	1.61	8.4	31.3	26	7.3
19$_{4-c}$			18.7*	×16	37	0.34	0.8	>45	45	15.3
20$_{4-a}$	4	plumbagin	1.7	×201	20	3.11	13.0	7.8	4.0	>1.5
20$_{4-b}$		(R$_1$ = OH)	2.5	×335	17	5.13	25.2	29.6	17.2	>1.3
20$_{4-c}$			0.45	×201	28	3.83	11.4	11.1	4.3	1.1
19$_{5-a}$	5	menadione	1.7	×69	21	1.2	4.8	5.4	4	2.6
19$_{5-b}$		(R$_1$ = H)	3.1	×33	12	0.47	3.3	14.3	11	5.7
19$_{5-c}$			2.5*	×8	3	0.09	2.3	22.8	12.5	>1.5
20$_{5-a}$	5	plumbagin	1.6	×221	37	5.91	13.3	34.8	24.4	0.3
20$_{5-b}$		(R$_1$ = OH)	1.6	×121	8	1.61	16.8	17.4	11.4	>1.3
20$_{5-c}$			2.0	×227	28	4.87	14.5	10.3	3.0	>1.4

[a] In the presence of 57 μM T(S)$_2$. [#] At 12.5 μM. *Precipitates in the assay buffer at the IC$_{50}$ value. [b] Reduction of the NQs by TcTR was measured at 25 °C in TR assay buffer, pH 7.25, at an NADPH concentration of 250 μM as described in the Experimental Section. The control assays which contained only NADPH and the enzyme represent the intrinsic oxidase activity of TR. Oxidation of NADPH was followed at 340 nm. The rate of NADPH oxidation by TcTR in the presence of 25 μM NQ was x-fold increased, when compared to the intrinsic oxidase activity of the enzyme. The values are the mean of at least two independent measurements which differed by less than 10%. [c] T/100 means the compound was toxic to macrophages, 100% inhibition; T/+ means the compound was toxic to macrophages but parasites were still present: [d] at 30 μM, [e] at 10 μM, [f] at 3 μM.

parasite and host enzymes (for menadione: IC$_{50}$ = 63 μM with hGR and 55 μM with TcTR; for plumbagin: IC$_{50}$ = 38 μM with hGR and 28 μM with TcTR). The most potent series of TR inhibitors **19−20** (n = 4−5) were also tested in the standard hTrxR screening assay using the recently reported 5,5′-dithiobis(2-nitrobenzamide) (DTNBA) as an alternative substrate for hTrxR[39] and in the standard hGR screening assay using GSSG as substrate. At 25 μM NQ and 200 μM disulfide substrate, both assays indicated a selective affinity of compounds **20$_{4-c}$** and analogues for the trypanosomal enzyme compared to human GR and TrxR (data not shown).

Reduction of NQ Derivatives by TcTR and hGR. Three series of NQs (menadione, plumbagin, and juglone derivatives) were studied as subversive substrates of TR by following the oxidation of NADPH in the presence of 25−100 μM NQ. The NQ reductase activity of TcTR (eq 2) was compared with the intrinsic NADPH oxidase activity of the enzyme in the absence of NQ (eq 1). The data represent the increase of the rate of NADPH oxidation (x-fold) in the presence of 100 μM

compounds **3−6**, **16−18** (Table 1) or 25 μM compounds **19−20** (Table 3).

$$2O_2 + NAD(P)H + H^+ \xrightarrow{\text{enzymatic}}$$
$$2O_2^{-\bullet} + NAD(P)^+ + 2H^+ \quad (1)$$

$$2NQ + NAD(P)H + H^+ \xrightarrow{\text{enzymatic}}$$
$$2NQ^{-\bullet} + NAD(P)^+ + 2H^+ \quad (2)$$
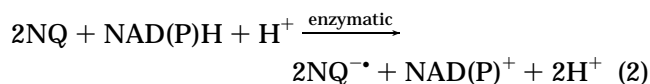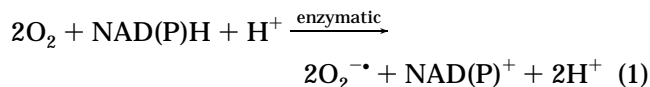
For the first series of 3-polyamino-1,4-NQ derivatives **3−6** (Table 1), redox cycling activity proved to be lower (2.0−6.4-fold) than that observed at 100 μM unsubstituted menadione (17-fold) and plumbagin (39-fold). This may be due to the electron-donating effect of the nitrogen atom bound directly to the quinone moiety. Among the 3-(polyaminocarbonylalkyl)-1,4-NQs **16−17** (Table 1), only **16$_{2-g}$** (19-fold) displayed an NADPH oxidase activity comparable with that of menadione. In the plumbagin and juglone series, **17$_{2-g}$** (38-fold), **17$_{3-f}$** (40-fold), and **18$_{3-f}$** (45-fold) showed NADPH oxidase activities comparable with that of plumbagin. **18$_{3-g}$**
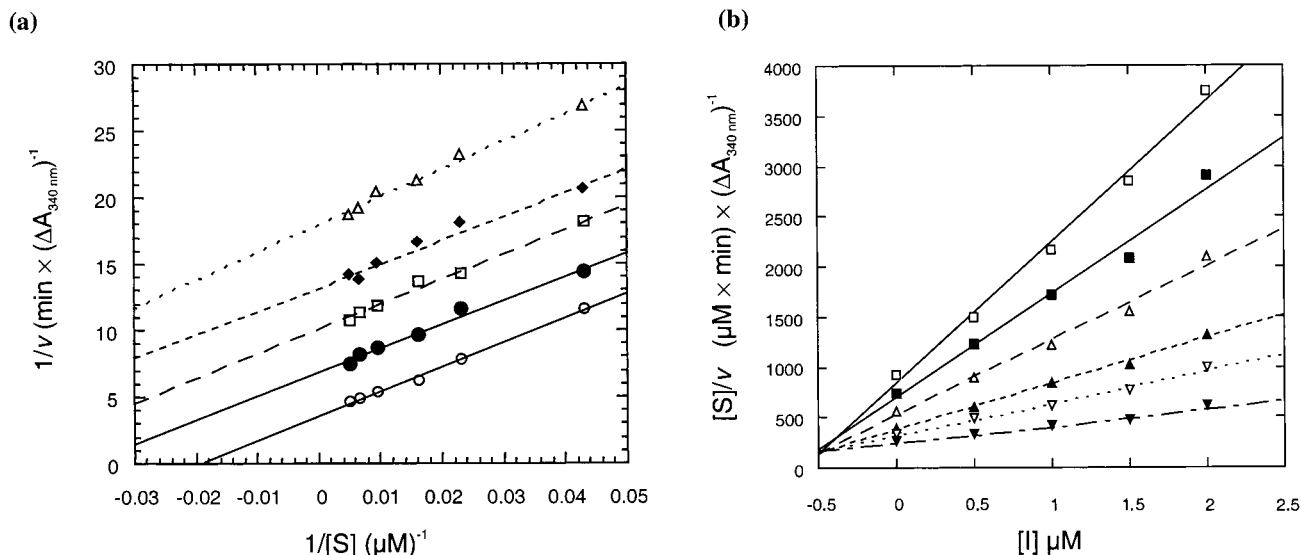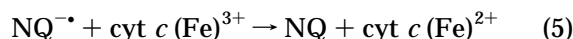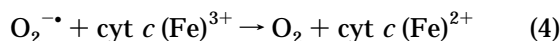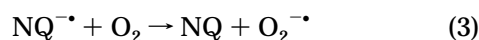
(a)

(b)

Figure 1. Lineweaver–Burk plot of $1/v$ versus $1/[S]$ (a) and Cornish–Bowden plot of $[S]/v$ versus $[I]$ (b) for the uncompetitive inhibition of TcTR by 20_{4-c} against T(S)$_2$. The assays were measured at 22 °C at a constant concentration of 200 μM NADPH and varying concentrations of **204-c** 0 (○), 0.5 (●), 1.0 (□), 1.5 (◆), 2.0 (△) μM. The concentrations of T(S)$_2$ were 23 (▼), 43 (▽), 62 (▲), 103 (△), 151 (■), 201 (□) μM. All assays contained a final concentration of 1% DMSO. The reaction was started by adding enzyme (10^{-2} units in a total volume of 500 μL), and NADPH consumption was followed.

caused the highest NQ reductase activity (220-fold). In comparison with the mono-NQ derivatives, the 3,3′-[polyaminobis(carbonylalkyl)]bis(1,4-NQ)s **19−20** (Table 3) were much more effective subversive substrates of TcTR. The rate of NADPH oxidation by TcTR increased 8−117-fold in the presence of 25 μM menadione derivatives **19**, when compared to the intrinsic NADPH oxidase activity of the enzyme. Under identical conditions, the rate of NADPH oxidation by TcTR increased 83−335-fold in the presence of the corresponding plumbagin derivatives. The K_m and k_{cat} values were derived from measurements at five different concentrations of NQ. To gain insight of where the NQ reduction takes place in the enzyme, we measured the reduction of 20_{4-c} in the presence of mepacrine, a known competitive inhibitor of T(S)$_2$ reduction.[40] Only a partial inhibition was detected at 50 and 100 μM mepacrine in the presence of varying concentrations of 20_{4-c} (3−50 μM), which may be an indication that the disulfide binding site of TR is not the major binding site of the bis(NQ) 20_{4-c}.

The efficiency of NQs as turncoat inhibitors of TR can be defined by the ratio $(k_{cat}/K_m)/IC_{50}$, combining the redox cycling activity and inhibition of the physiological reaction of TR. 20_{4-c} was the most potent TcTR turncoat inhibitor with the highest $(k_{cat}/K_m)/IC_{50}$ value equal to 25.3×10^{10} M^{-2} s^{-1}. Production of superoxide anion radicals by this compound (eq 3) was evaluated by coupling reaction 2 to cytochrome c (Fe^{3+}) reduction (eqs 4 and 5).

$$\text{NQ}^{-\bullet} + \text{O}_2 \rightarrow \text{NQ} + \text{O}_2^{-\bullet} \qquad (3)$$

$$\text{O}_2^{-\bullet} + \text{cyt } c \text{ (Fe)}^{3+} \rightarrow \text{O}_2 + \text{cyt } c \text{ (Fe)}^{2+} \qquad (4)$$

$$\text{NQ}^{-\bullet} + \text{cyt } c \text{ (Fe)}^{3+} \rightarrow \text{NQ} + \text{cyt } c \text{ (Fe)}^{2+} \qquad (5)$$

Addition of SOD in the presence of 12.5 μM 20_{4-c} decreased the rate of cytochrome c reduction by **88%**, which confirmed that reduction of 20_{4-c} by TR generates

superoxide anion radicals. A comparison of the amount of cytochrome c reduced (measured at 550 nm) per oxidized NADPH (measured at 340 nm) in the presence of 12.5 μM 20_{4-c} yielded a 1:2 ratio (7.1 and 3.5 μmol/min/mg, respectively).

To assess the preference of 20_{4-c} as subversive substrate of TcTR over hGR, the NQ reductase activity was measured in the cytochrome c reduction assay with hGR in the presence of 12.5 μM 20_{4-c} and compared with that observed in the presence of 12.5 μM plumbagin. The rate of cytochrome c reduction was not significantly increased (1.1-fold) in the presence of 20_{4-c}, when compared to that in the absence of NQ, which confirmed that hGR does not reduce 20_{4-c}. Under identical conditions, the rate of cytochrome c reduction increased 1.6-fold in the presence of the parent plumbagin.

Modeling Studies. The crystallographic analysis of hGR has revealed that certain un/noncompetitive inhibitors bind in a cavity distinct from the disulfide and NADPH binding sites.[25−29] This "third site" is situated at the 2-fold symmetry axis of the homodimeric protein[25] and is the locus of binding of 2-methyl-1,4-NQ (menadione),[26] 3,7-diamino-2,8-dimethyl-5-phenylphenazinium chloride (safranin),[26] 6-hydroxy-3-oxo-3H-xanthene-9-propionic acid,[27] a series of 10-arylisoalloxazines,[28] and S-(2,4-dinitrophenyl)glutathione.[29] As shown in Figure 2, the structurally closely related parasite enzyme TcTR (35% sequence identity with hGR) possesses a similar cavity. To elucidate possible discriminating factors between the "third sites" in the human and parasite enzymes, a detailed analysis has been undertaken based on the available structural data.

In TcTR, the cavity is lined by 32 residues (Table 4) of each monomer (41 in hGR). 27 of these residues are conserved in all TRs of *Crithidia fasciculata, Trypanosoma brucei, Trypanosoma congolense,* and *Leishmania donovani*, suggesting a common mode of interaction with molecules probably binding in this cavity. In contrast, only 15 residues are conserved when comparing TcTR with hGR. Moreover, none of the residues
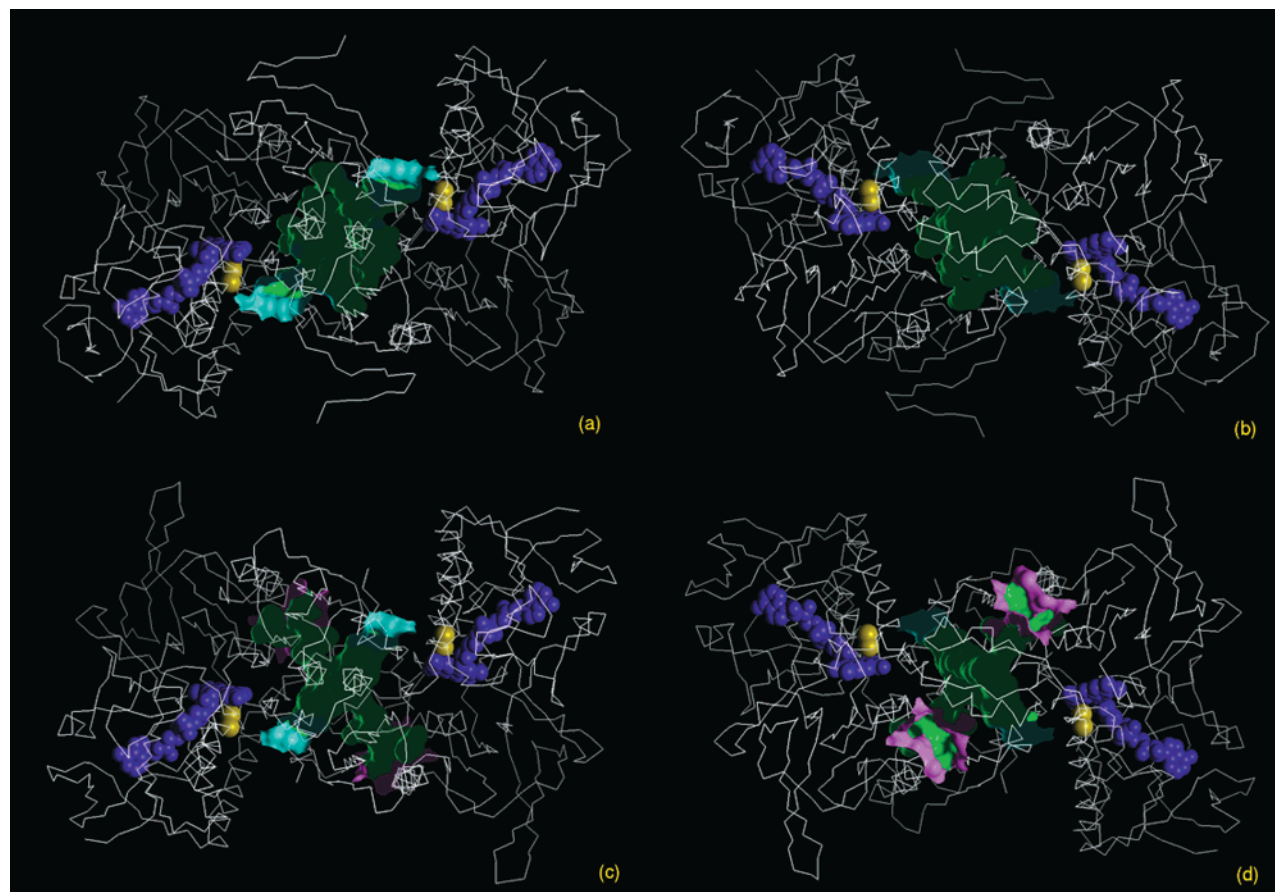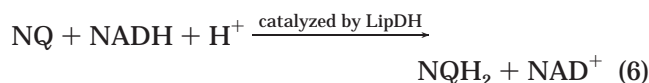
Figure 2. Front (a,c, respectively) and back (b,d, respectively) views of the protein backbone depicted for TcTR and hGR, showing the cavity at the dimer interface (green area). The cavity, also called "third site", is connected to the two disulfide substrate ($T(S)_2$ and GSSG, respectively) binding sites through two short channels (blue area). These channels emerge at the bottom of the V-shaped catalytic crevices in close proximity to the redox-active disulfide bridges. As indicated by the CAST calculation, two additional channels which connect the cavity with the protein surface in a region distinct from the two catalytic sites are detectable in the hGR structure (pink area). The redox-active disulfide bridges (Cys53 and Cys58 in TcTR; Cys58 and Cys63 in hGR) and the FAD molecules are given as yellow and purple hard spheres, respectively.

involved in the binding of xanthene derivatives to hGR (Trp70, Asn71, Val74, His75, Phe78, Met79, His82, and Tyr407)[27] is conserved in the five TR sequences. Figure 3 shows specific residues in the "third site" of TcTR. A summation of net charges of acidic (−I) and basic (+I) residues, considering histidine residues in their unprotonated state, leads to an overall charge of −IV for the interfacial cavity TcTR and only −II for hGR. Remarkable is the high number of histidine residues in the cavity of human GR with a total of 5/monomer while TcTR has only 2/monomer. With regard to residues that could be specifically involved in the binding of ligands, Thr66, Gln69, Tyr70, Gln242, Ile369, Met400, Lys409, Phe411, Asp432, and Pro435 are conserved in the different TRs but not in hGR. Gln69, Met400, and Asp432 are particularly accessible inside the interface cavity and are characterized by high thermal parameters in the structure of free TcTR.[41]

As shown in Figure 2a,b, the "third site" of TcTR is almost globular while that of hGR (Figure 2c,d) has a rather cross-shaped form. The molecular surface and volume of the cavity calculated with the CAST software are 1755 Å² and 2280 Å³ in TcTR and 1954 Å² and 2399 Å³ in hGR. The surface and volume accessible to solvent are 888 Å² and 511 Å³ (887 Å² and 464 Å³ in hGR), respectively. The interface pocket of both enzymes is connected to the two disulfide substrate binding sites

through short channels. There is no direct connection with the FAD and NADPH binding sites. These "primary" channels open into the catalytic sites near the redox-active disulfide bridges. The circumference of these channel openings of TcTR enzyme is about 31 Å, and the molecular area is about 46 Å². The openings are delineated by hydrophobic residues (Phe396, Pro398, Leu399, Pro462, Thr463, and Val59′ of the other subunit) strictly conserved in the different TRs. In hGR, a unique substitution is observed, Leu399 of TcTR being replaced by Met406. In the structure of TcTR without bound ligands,[41] Phe396, Pro398, and Leu399 at the opening exhibit particularly high *B*-factors of 40−60 Å². Each channel opening is 14 Å apart from the center of the cavity, and its distance to the redox-active disulfide bridge is about 9−10.5 Å, the shortest distance between the catalytic sulfur atoms and atoms at the channel entrance being 4.4 Å. In hGR, the CAST calculation identified two additional channels, explaining the higher number of residues lining the cavity (41/monomer in hGR versus 32/monomer in TcTR). These "secondary" channels provide direct access to the surface of the protein in a region distinct from the two catalytic sites. By neglecting the residues involved in these regions, the structural comparison of the cavities in the human and parasitic enzymes by superposition of main chain atoms yielded a root-mean-square (rms) deviation of 0.91 Å.

Reduction of Menadione Derivatives by *T. cruzi* and Pig Heart LipDH. The ability of LipDH to reduce menadione is well-known since the yeast enzyme was first described as menadione reductase.[42] Reduction of the menadione derivatives was first studied by following the oxidation of NADH which yields the sum of one- and two-electron reduction rates of the compounds (eqs 2 and 6). As presented in Table 5, the unsubstituted menadione is reduced by the parasite enzyme with a k_{cat}/K_m value of 1×10^5 M^{-1} s^{-1}. The best new derivative was **14$_3$** which in the case of TcLipDH showed a catalytic efficiency almost as high as that of menadione. To estimate the amount of semiquinone formed in the LipDH-catalyzed reduction of NQs, the reaction was coupled to cytochrome *c* reduction as described for TR (eqs 2−5). The assays were carried out at a constant concentration of 50 μM NQ since at higher concentrations the comproportionation of hydronaphthoquinones (NQH$_2$) and oxidized NQ may become significant (eqs 6−7).

$$\text{NQ} + \text{NADH} + \text{H}^+ \xrightarrow{\text{catalyzed by LipDH}} \text{NQH}_2 + \text{NAD}^+ \quad (6)$$

$$\text{NQH}_2 + \text{NQ} \rightarrow 2\text{NQ}^{-\bullet} + 2\text{H}^+ \quad (7)$$

This nonenzymatic generation of semiquinones can give rise to an erroneously high cytochrome *c* reductase activity.[3] At concentrations lower than 50 μM, reduction of the NQ by TcLipDH was too slow to allow detailed kinetics. Therefore the rate of cytochrome *c* reduction was measured in the presence of 50 μM NQ and compared with the rate of NADH oxidation at the same concentration (Table 5). Under these conditions TcLipDH catalyzed the one-electron reduction of the menadione derivatives with an efficiency of about 50%. SOD diminished the rate of cytochrome *c* reduction by 83% in the case of **9$_2$** and **16$_{2-f}$** and by 67% in the presence of menadione, which confirms the generation of superoxide anion radicals. The compounds **3$_b$** and **3$_f$** and the bis(NQ) derivative **6$_c$** underwent very little or no reduction at all by TcLipDH (see structures in Table 1). Only **6$_c$** at 250 μM enhanced the rate of NADH oxidation by about 25%. K_m and V_{max} values were not determined. The apparent second-order rate constants for the reduction of the menadione derivatives by pig heart LipDH were similar to the values obtained with the parasite enzyme (Table 5). Again the unsubstituted menadione was the most effective substrate. Also in the case of the mammalian enzyme a lower K_m value was always accompanied by a lower V_{max} value. The proportion of one-electron reduction ranged from 21−84% of the total electrons transferred from NADH to NQ. SOD diminished the rate of cytochrome *c* reduction by 86% in the case of **9$_2$** and by 35% in the case of menadione. Reduction of cytochrome *c* mediated by **16$_{2-f}$** was completely inhibited by SOD.

Reduction of Plumbagin Derivatives by *T. cruzi* and Pig Heart LipDH. In the series of plumbagin derivatives, the unsubstituted compound also proved to be the best substrate of both LipDHs (Table 5). When following NADH consumption, plumbagin was reduced by TcLipDH with a k_{cat}/K_m of 4.8×10^5 M^{-1} s^{-1}. Of the newly synthesized derivatives, **15$_3$** with 2.3×10^5 M^{-1}

Table 4. Residues Lining the Interface Cavity of TcTR and the Corresponding Residues in Other TRs and hGR[a]

TcTR		rel acc[b] (%)	TbTR	TcgTR	CfTR	LdTR	hGR
V59	o	15					**V64**
K62		32					**K67**
L63		3					V68
V65		7					W70
T66		13					N71
Q69		31			N		V74
Y70		3					H75
E72		4	D	D	D	D	**E77**
H73		27	H	Q	T	L	F78
E76		4					D81
Q242		1					E237
F367		10					**F372**
S368		1					**S373**
I369		10					H374
P370		5					**P375**
P371		10					**P376**
F396		37					**F403**
P398	o	21					**P405**
L399	o	32					M406
M400		37					Y407
H401		4					**H408**
K409		7					T415
T410		31	K	K	K	E	K416
F411		2					C417
G431							**G437**
D432		45					L438
N433		42	G	S	S	S	G439
P435		14					D441
E436		16					**E442**
P462	o	2					**P468**
T463	o	22					**T469**
S464		22					**S470**

[a] Residues conserved between TRs and hGR are given in bold letters (residues corresponding to "secondary" channels in hGR are not listed). The numbering used for TcTR residues refers to that of the three-dimensional structure accessible at the Protein Data Bank under 1aog refcode.[41] For the different TRs, only mutations are specified. o denotes TcTR residues at the channel openings. [b] Relative accessibilities of side chains, e.g. surface$_{real}$/surface$_{max}$ ratios as estimated by using the NACCESS software.[66]

s^{-1} showed the highest catalytic efficiency. The parasite enzyme reduced compound **10$_2$** almost as effectively as plumbagin, yet the much higher K_m value for this derivative resulted in a relatively low k_{cat}/K_m ratio. When studied in the cytochrome *c* assay, plumbagin yielded 80% one-electron reduction which was completely abolished in the presence of SOD. The derivatives **14$_3$** and **15$_3$** caused a cytochrome *c* reduction in the absence of LipDH and thus could not be studied for their one-electron reduction capacity. Reduction of **17$_{2-f}$** and **10$_2$** by TcLipDH occurred 50% and 66% as one-electron reductions, respectively, and SOD diminished the rate of cytochrome *c* reduction by about 75%. Also pig heart LipDH exhibited the highest catalytic efficiency with the unsubstituted plumbagin resulting in a k_{cat}/K_m of 2.9×10^5 M^{-1} s^{-1}. Interestingly, the mammalian enzyme had a much lower activity with the newly synthesized derivatives than the parasite enzyme. For instance, reduction of **15$_3$** occurred at a rate only one-seventh that of the parasite enzyme. The apparent second-order rate constants for **15$_3$**, **17$_{2-f}$**, and **10$_2$** were about an order of magnitude lower than that for plumbagin. The proportion of one-electron reduction ranged from 38% to 89%, and the reactions were inhibited by SOD between 50% and 90%.

Antitrypanosomal Activities. Antitrypanosomal activities of the compounds toward the intracellular
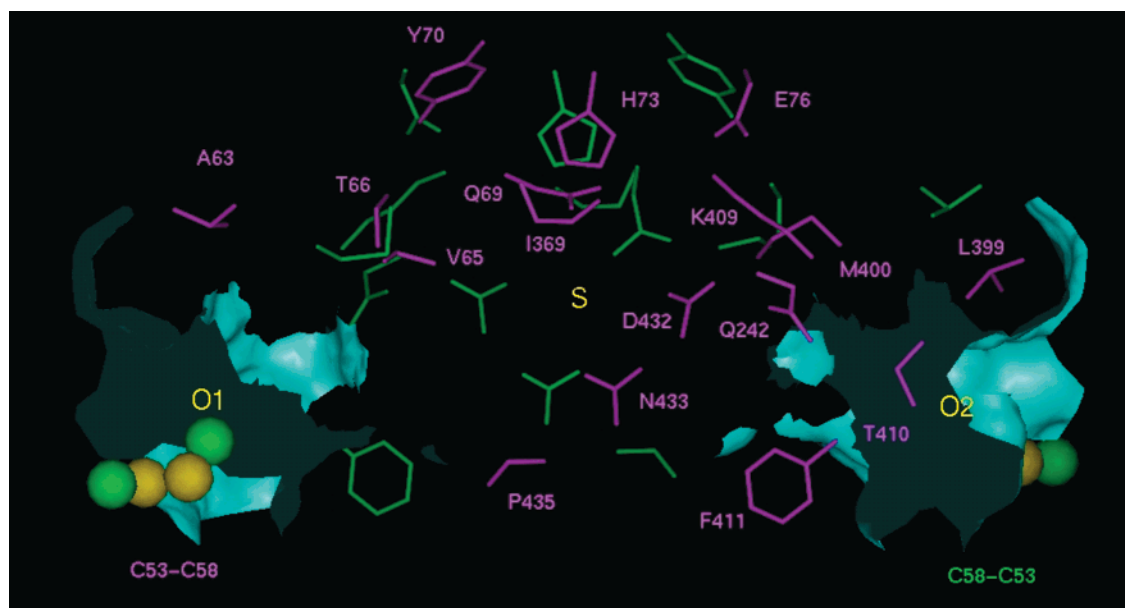
Figure 3. Enlarged view of the "third site" in TcTR with its connecting channels and corresponding openings. Only residues specific to the parasite enzyme are shown (side chain); those common to human GR have been omitted. The two identical subunits are pink and green. S, O1, and O2 designate the centers of the cavity and of the channel openings, respectively. Each channel entrance is 14 Å away from the center of the cavity (S–O1 and S–O2 distances), and the distance between the two entrances is 27 Å (O1–O2 distance). The approximate distance between the center of the entrances (O1 or O2) and the redox-active cysteine residues (Cys53 and Cys58) is 9–10.5 Å. The side chains of active cysteine residues are depicted as yellow (S_γ atoms) and green (C_β atoms) ball-and-sticks.

Table 5. 1,4-NQ Derivatives Studied as Subversive Substrates of LipDH from *T. cruzi* and Pig Heart

9_2 R = H
10_2 R = OH

14_3 R = H
15_3 R = OH

16_{2-f} R = H
17_{2-f} R = OH

	TcLipDH				pig heart LipDH			
	NADH oxidation[a]			cyt *c* reduction: NADH oxidation, (μmol/min/mg): (μmol/min/mg)[b]	NADH oxidation[a]			cyt *c* reduction: NADH oxidation, (μmol/min/mg): (μmol/min/mg)[b]
compd	K_m (μM)	V_{max} (μmol/min/mg)	k_{cat}/K_m (10^4 M^{-1} s^{-1})	(% one-electron reduction)	K_m (μM)	V_{max} (μmol/min/mg)	k_{cat}/K_m (10^4 M^{-1} s^{-1})	(% one-electron reduction)
menadione	170	21.04	10	12.7:13.5 (47)	72	11.5	13	8.1:4.8 (84)
9_2	85	6.73	6.6	3.0:2.7 (56)	40	1.52	3.2	0.5:1.2 (21)
14_3	20	2.02	8.4	*c*	25	1.03	3.4	*c*
16_{2-f}	90	3.21	3	1.6:1.7 (47)	110	3.46	2.6	0.8:0.8 (50)
plumbagin	40	22.9	48	26.1:16.3 (80)	74	25.3	29	15.4:10.0 (77)
10_2	140	17.2	10.2	6.6:5.0 (66)	75	2.2	2.4	1.6:0.9 (89)
15_3	30	8.24	23	*c*	40	1.66	3.5	*c*
17_{2-f}	20	2.72	11.3	1.9:1.9 (50)	15	1.09	6.1	0.6:0.8 (38)

[a] NADH oxidation was followed at 31 °C in 50 mM potassium phosphate, 1 mM EDTA, pH 7.0, at a constant concentration of 100 μM NADH. The NQs were varied between 10 μM and 1.2 mM. The K_m and k_{cat} values were derived from Lineweaver–Burk plots. [b] Cytochrome *c* reduction was measured at 100 μM NADH, 50 μM cytochrome *c*, and 50 μM NQ in 50 mM potassium phosphate, pH 7.0. NADH oxidation was followed under identical assay conditions lacking cytochrome *c*. [c] The compound could not be measured in the cytochrome *c* assay because of a direct reduction of cytochrome *c*. All assays were carried out at least in duplicate, the values varied by less than 8%. The intrinsic oxidase activity of *T. cruzi* LipDH is 1.2 μmol/min/mg when following NADH oxidation which corresponds to about 0.6% of the LipDH activity. In the reaction coupled to cytochrome *c* the activity is 0.7 μmol/min/mg. The latter reaction is completely inhibited by SOD. The oxidase activity of pig heart LipDH in the NADH assay is 0.8 μmol/min/mg (which corresponds to 0.4% of LipDH activity) and 0.4 μmol/min/mg in the cytochrome *c* assay. The latter activity is also completely abolished by SOD.

amastigote stage of both *T. cruzi* and *L. donovani* (or *L. infantum*) and upon the *T. brucei* bloodstream form trypomastigotes are given in Tables 1–3, as ED$_{50}$ values (when these could be calculated). Taking into account the sensitivity of the different parasites, compounds having ED$_{50}$ values below 5 μM with *T. cruzi* or *L.*

donovani and values below 1 μM with *T. brucei* can be considered as trypanocidal lead molecules. The standard drugs, nifurtimox and pentamidine, were used as positive controls for *T. cruzi* and *T. brucei* and displayed ED$_{50}$ values in the range 2.2–4.4 and 0.03–0.1 μM, respectively. The 3-polyamino-1,4-NQs **3–6**, the 3-(poly-
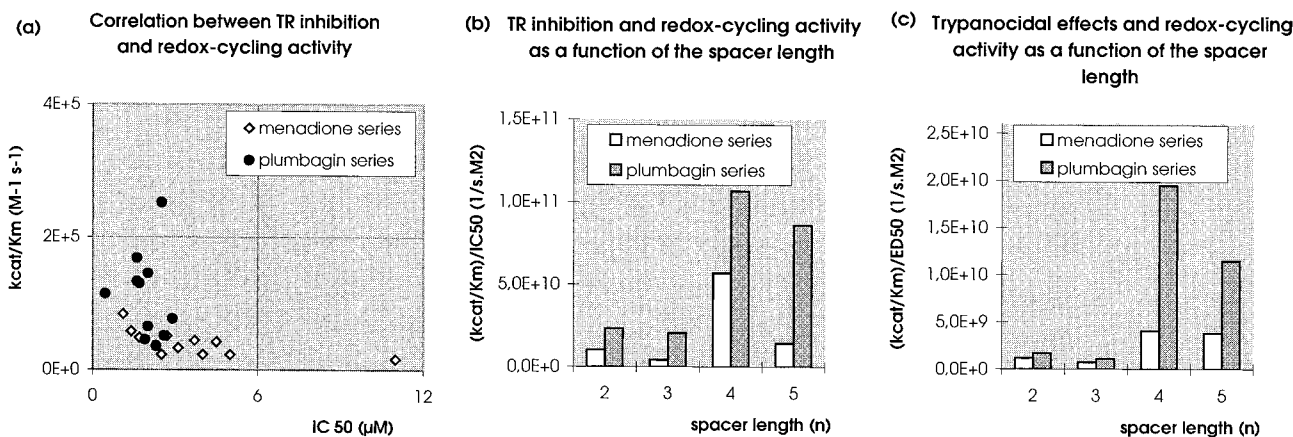
Figure 4. Influence of the spacer length on inhibition of T(S)$_2$ reduction, redox cycling activity, and trypanocidal effects of the 3,3′-[polyaminobis(carbonylalkyl)]bis(1,4-NQ)s **19−20** of the menadione and plumbagin series: (a) correlation between TR inhibition and redox cycling activity; (b) TR inhibition and redox cycling activity as a function of the spacer length *n*; (c) trypanocidal effects and redox cycling activity as a function of the spacer length *n*.

aminocarbonylalkyl)-1,4-NQs **16−17**, the 2,3-bis(polyaminocarbonylalkyl)-1,4-NQ **18** (Table 1), and the starting acid derivatives **9−11** (Table 2) exerted weak trypanocidal effects upon the different trypanosomatids in corroboration with an observed weak TcTR inhibition or, alternately, a cytotoxicity displayed upon human macrophages. The cytotoxic effects of polyamine derivatives upon human cells has often been encountered.[43,44] When molecules **3−6** proved noncytotoxic upon human macrophages, the weak antitrypanosomal action could be related to a low production of superoxide anion radicals in agreement with the redox potential of the molecule, affected by the donor effect of the nitrogen atom linked directly to the quinone moiety. In contrast, the 3,3′-[polyaminobis(carbonylalkyl)]bis(1,4-NQ)s **19−20** (Table 3) displayed significant antitrypanosomal effects, especially toward *T. cruzi*. Several derivatives yielded ED$_{50}$ values of 3−4 μM (see compounds **20$_{4-a}$**, **20$_{4-c}$**, **19$_{5-a}$**, **20$_{5-c}$**) comparable to that of nifurtimox. *T. brucei* and *L. donovani* were less sensitive to these 1,4-NQ derivatives, with ED$_{50}$ values for *T. brucei* around 1 μM (see compounds **20$_{4-c}$**, **20$_{5-a}$**), and *L. donovani*, with ED$_{50}$ values of about 5 μM for the most active compound (see compound **19$_{5-a}$**). As expected, the data revealed a clear tendency within the three series of 1,4-NQ derivatives designed in Chart 1: the most potent TcTR inhibitors (**19−20**: IC$_{50}$ values below 5 μM) were the most active antitrypanosomal compounds. It should be noted that no cytotoxicity upon human macrophages was observed above 25 μM for the compounds of this **19−20** series. Nevertheless, within this last series (Table 3), there was no straight correlation between ED$_{50}$ values from in vitro antitrypanosomal assays and IC$_{50}$ values from TS$_2$ reduction assays. The highest antiparasitic activity within the 3,3′-[polyaminobis(carbonylalkyl)]bis(1,4-NQ)s **19−20** was observed with those compounds possessing the longest spacer between the two NQ moieties (*n* = 4−5). This finding suggests that physical and molecular features other than TR binding must be considered, for instance the hydrophobicity of a long alkyl chain which may facilitate cellular penetration. A second parameter that is likely to play an important role for the trypanocidal activity of the most potent derivatives is the specific release of

superoxide anions radicals in the parasites, due to the redox cycling activity of the NQs.

In addition, the starting *N*-Boc-protected amine derivatives **14−15** (Table 2) displayed potent trypanocidal effects upon *T. cruzi* and *T. brucei* with ED$_{50}$ values for *T. cruzi* around 3−4 μM for the most active compounds (see compounds **14$_5$**, **15$_2$**, **15$_3$**) and around 1 μM for *T. brucei* (see compounds **14$_2$**, **15$_2$**, **15$_3$**, **15$_4$**). The unexpected lack of TcTR inhibition by this series of 1,4-NQ indicates the presence of other targets responsible for the observed antitrypanosomal activities.

Correlation between Redox Cycling Activities and in Vitro Antitrypanosomal Activities. In the 3,3′-[polyaminobis(carbonylalkyl)]bis(1,4-NQ) series **19−20**, the role of the parent NQ, the nature of the polyamine, and the chain length were analyzed with respect to the redox cycling properties of each derivative. Some structure−activity relationships (SARs) for the inhibition of T(S)$_2$ reduction and redox cycling activities could be derived (Figure 4). The highest redox cycling activities correlate with strong inhibition of the physiological T(S)$_2$ reduction, particularly in the plumbagin series (Figure 4a). For each group of three polyamine derivatives (**19$_{2a-c}$**, **19$_{3a-c}$**, **19$_{4a-b}$**, **19$_{5a-c}$**, **20$_{2a-c}$**, **20$_{3a-c}$**, **20$_{4a-c}$**, **20$_{5a-c}$** in Table 3) the mean values of the ratio of (k_{cat}/K_m)/IC$_{50}$ determined from the NADPH oxidase assay and the T(S)$_2$ reduction assay were calculated (Figure 4b), as were the mean values of the ratio of (k_{cat}/K_m)/ED$_{50}$ determined in the NADPH oxidase assay and the *T. cruzi* trypanocidal tests (Figure 4c). From these data, an effect of the spacer length can be deduced. When TR inhibition, redox cycling activity of TR, and trypanocidal activities were expressed as a function of the spacer length, structure−activity curve profiles attained a maximum when *n* = 4 in both the plumbagin and menadione series (Figure 4b,c, respectively). Interestingly, plumbagin derivatives showed much higher activities than their menadione counterparts (Figure 4b,c), which is in agreement with the one-electron reduction potentials of the parent molecules (E_1 values = −0.20 and −0.16 V for menadione and plumbagin, respectively).[17]

Three menadione and three plumbagin derivatives displaying potent trypanocidal effects and no TR inhibition were also examined as redox cycling substrates of

LipDH, another flavoenzyme characterized from *T. cruzi*.[14] As observed with the positively charged nitrofuran chinifur, no inhibition of dihydrolipoamide dehydrogenation and relatively weak redox cycling activities were found with menadione and plumbagin derivatives carrying positively or negatively charged substituents (**9₂**, **10₂**, **16₂₋f**, **17₂₋f**). Interestingly, the most efficient substrates of TcLipDH were the uncharged carbamates **14₃** and **15₃** which displayed potent antitrypanosomal activities against *T. brucei* and *T. cruzi* in culture but no inhibition of TR.

Discussion

The aim of this study was to develop new NQs that are specific and potent inhibitors of TcTR and are reduced by the enzyme via a one-electron mechanism leading to the generation of superoxide anion radicals. The data obtained from the chemical synthesis and enzymatic studies revealed that it is possible to design specific and potent TcTR inhibitors from a lead structure, i.e. menadione and plumbagin, known to interact with numerous NADPH-dependent disulfide oxidoreductases, like hGR, TcTR, and hTrxR. The chemistry which has been developed has led to several building blocks in the 1,4-NQ series, **9−11**, which can easily be derivatized with structurally diverse amines. This chemistry has enabled us to design a series of 1,4-NQs, substituted by amino side chains at C-2 and C-3 of the quinone moiety of three natural 1,4-NQs, namely menadione, plumbagin, and juglone already known for their trypanocidal activities but lacking in specificity. Optimization of TcTR inhibition and TcTR specificity versus human disulfide reductase specificities was achieved with the 3,3′-[polyaminobis(carbonylalkyl)]bis(1,4-NQ) **19−20** series, characterized by an optimal chain length between the two NQ moieties ($n = 4−5$). The results presented in this paper suggest that inhibition of the $T(S)_2$ reduction alone is not sufficient for a strong trypanocidal activity, as illustrated with several 3-polyamino-1,4-NQs (**3b**, **6c**, **6d**) or 3,3′-[polyaminobis(carbonylalkyl)]-bis(1,4-NQ)s (**19−20**; $n = 2$ or 3), displaying IC₅₀ values below 10 μM. Indeed, the crucial parameter for a high trypanocidal activity appears to be the combination of both redox cycling activity and inhibition of $T(S)_2$ reduction. This point is clearly illustrated by the properties of the 3,3′-[polyaminobis(carbonylalkyl)]-bis(1,4-NQ) (**20**; $n = 4$ or 5). The plumbagin derivatives with $n = 4$ were the most efficient subversive substrates of TcTR, were the most potent inhibitors of the TR-catalyzed $T(S)_2$ reduction, and displayed the strongest trypanocidal effects toward *T. cruzi* cultures. These compounds combined the highest ratio $(k_{cat}/K_m)/IC_{50}$ (mean value from **a−c** derivatives = 10.7×10^{10} M^{-2} s^{-1}) with the highest ratio $(k_{cat}/K_m)/ED_{50}$ (mean value from **a−c** derivatives = 1.9×10^{10} M^{-2} s^{-1}). Also in the menadione series, derivatives with $n = 4$ showed maximum $(k_{cat}/K_m)/IC_{50}$ and $(k_{cat}/K_m)/ED_{50}$ mean values of 5.7×10^1 and 0.4×10^{10} M^{-2} s^{-1}, respectively. However, the menadione derivatives were much less efficient subversive substrates than the corresponding plumbagin derivatives, which also correlated with lower antitrypanosomal activities and the redox potentials of the parent molecules. Analyzing the structural features of the NQ derivatives, our studies revealed that the presence of a long alkylamino chain linking the two

quinone moieties is essential for both $T(S)_2$ reduction inhibition and redox cycling activity. In addition, the presence of protonatable amino groups in the spacer is indispensable for TR recognition. Interestingly, *N,N*-bis-acylated polyamine derivatives are also potent and specific inhibitors of TR from *T. cruzi* and *Crithidia fasciculata*, i.e. the *N,N*-1,5-pentylenediamide and N^4,N^8-bis-acylated spermidine derivatives with 2-aminodiphenyl sulfide substituents[45,46] as well as kukoamine A,[47] respectively. The bis(NQ) compounds presented in this paper are structurally related to kukoamine A, a potent mixed-type competitive TR inhibitor.[47] Kukoamine A (N^1,N^{12}-bis(dihydrocaffeoyl)spermine), composed of two catechol moieties linked by a 20-atom diacylspermine chain, has been suggested to act through its orthohydroquinone state as a subversive substrate of TR. The mode of inhibition of the enzyme by kukoamine A and by bis(NQ) derivatives could be in fact very similar. Recently, a crystallographic study of TR crystals soaked in a saturating solution of kukoamine A did not yield the binding site of the compound but indicated reduction of the active site disulfide bridge and probably a modification of Cys52 (Cys53 in our amino acid numbering, see Table 4).[48]

Subversive substrates (turncoat inhibitors) of TR and GR divert electrons from the physiologically catalyzed reactions. Reduction of such molecules may occur at the active site[49] or at different site(s) as already suggested for reversible inhibitors such as nitrofuran[37] and quinone.[17] In the case of the garlic-derived ajoene, the compound reacts with the two-electron reduced enzymes leading to a mixed disulfide at Cys58 (in hGR) and to an increased NADPH oxidase activity of the modified enzymes resulting in superoxide anion radical production.[49] This result fits with those obtained by Cenas and co-workers who reported that TR alkylated by iodoacetamide at Cys52 maintained considerable quinone reductase activity in the presence of juglone.[17] As TR follows a ping-pong reaction mechanism,[11,50] the uncompetitive inhibition type observed for numerous nitrofurans and quinones,[37] and in particular for the bis(NQ) **20₄₋c** studied here, may indicate the accumulation of dead-end NADP⁺·TR·T(S)₂ complexes.[51] However, the binding mode of these compounds in TR is not yet known. So far only one crystal structure of a TR/inhibitor complex has been elucidated, namely with the competitive inhibitor mepacrine.[40] While no structure of un/noncompetitive subversive substrate/TR complexes is available, the structures of several complexes between hGR and un/noncompetitive ligands have been described in detail.[26−29] These structures revealed that the inhibitor molecules bind in a large cavity present at the dimer interface, which is distinct from the GSSG, FAD, and NADPH binding sites. Binding of these ligands at this "third site" causes inhibition of the physiological GSSG reduction, but none of the compounds is reduced by hGR. In addition, ligands can have more than one binding site, as illustrated for menadione which binds to a lesser extent also at the NADPH and disulfide sites in hGR,[26] or as recently reported for acridine derivatives in TcTR.[52] Therefore it is tempting to speculate that the respective "third site" in TR is the binding site of the NQ molecules. The electron-transfer mechanisms operating between the flavin and NQ remain speculative

until structural studies will reveal if the compounds are reduced at the NADPH site, the $T(S)_2$ site, or the "third site". To gain insight in the locus where the NQ reductase activity may take place, reduction of 20_{4-c} was measured in the presence of mepacrine which acts as a competitive inhibitor of TR versus $T(S)_2$. Only little inhibition of NQ reduction was observed in the presence of up to 100 μM mepacrine. This result may indicate that the major binding locus of mepacrine in the $T(S)_2$ binding site is not the locus where the NQs are reduced, as postulated by Cenas and co-workers.[17]

A comparison of hGR and TcTR structures revealed that the respective cavities at the 2-fold axis of both enzymes have comparable dimensions but are clearly different in shape. Our studies gained insight in the accessibility of these cavities by a potential ligand. In both enzymes, the interface site is connected to the two catalytic sites by two short "primary" channels starting near the disulfide substrate binding sites. In hGR, two "secondary" channels were identified providing a direct access to the surface of the protein. Several residues in the cavity of TcTR show a marked flexibility, in particular those lining the "primary" channels which could be crucial for large ligands to reach the "third site".

With respect to the specificity toward TR, only 47% of the residues involved in the parasitic "third site" are conserved in hGR. The most striking finding is that none of the residues involved in the binding of un/noncompetitive hGR ligands is conserved in the five known TR sequences.[27] As mentioned previously,[9] the results obtained with the series of mono- and bis(NQ) derivatives show that the presence of amino groups is crucial for TR recognition. Under physiological conditions, these groups are positively charged and could correlate with the more pronounced acidity of the TcTR cavity (overall charge of $-$IV for TcTR versus $-$II for hGR). However this difference of charge must be considered with caution due to the presence of several histidine residues at the dimer interface. The preference of TR over hGR for positively charged ligands even if they bind at the "third site" may be due to the fact that the cavity at the 2-fold axis $-$ in contrast to hGR $-$ is obviously only accessible via the negatively charged TS_2 binding site. Comparison of the cavities may allow the prediction that, in particular, Asp432, Gln69, and Met400 may be important for ligand binding in TR. These residues are easily accessible and display high thermal parameters, as observed for Phe78 and Phe78′ in hGR which are directly involved in ligand binding.[26]

The lack of correlation between TR inhibition and the trypanocidal effects among several NQs (**14**−**15**) suggested a study of the redox cycling properties of several menadione and plumbagin representatives with LipDH, another flavoenzyme characterized in *T. cruzi*. Although the redox cycling activities of both carbamates **14**$_3$ and **15**$_3$ were lower than those of the unsubstituted menadione and plumbagin, the specificity of these derivatives for the parasite versus mammalian enzyme was much higher when compared with the parent molecules. The data are consistent with the possible development of potent and specific subversive substrates of TcLipDH as potential trypanocidal drugs, rendering the enzyme also an attractive target for antiparasitic chemotherapy.

In conclusion, the strong antitrypanosomal action of

several NQs, among the most efficient subversive substrates of TcTR and TcLipDH, suggest that NQ reduction leading to the generation of superoxide anion radicals is a promising strategy for the development of new trypanocidal drugs. The design and synthesis of more potent and specific NQs as turncoat inhibitors of TcTR or TcLipDH are in progress, with a focus on the preparation of new NQ moieties.

Experimental Section

Abbreviations: DMSO, dimethyl sulfoxide; DTNB, 5,5′-dithiobis(2-nitrobenzoic acid); DTNBA, 5,5′-dithiobis{*N*-[3-(dimethylamino)propyl]-2-nitrobenzamide}; GSH, reduced glutathione; GSSG, glutathione disulfide; GR, glutathione reductase; hGR, human glutathione reductase; HBTU, 2-(1*H*-benzotriazol-1-yl)-1,1,3,3-tetramethyluronium hexafluorophosphate; HOBt, *N*-hydroxybenzotriazole; LipDH, lipoamide dehydrogenase; TcLipDH, *Trypanosoma cruzi* lipoamide dehydrogenase; SOD, superoxide dismutase; Trx, thioredoxin; TrxR, thioredoxin reductase; hTrxR, human thioredoxin reductase; $T(SH)_2$, reduced trypanothione; $T(S)_2$, trypanothione disulfide; TR, trypanothione reductase; TcTR, *Trypanosoma cruzi* trypanothione reductase.

Enzymes. Recombinant TcTR (E.C. 1.6.4.8) was purified from *E. coli* SG5 cells carrying the overproducing expression vector pIBITczTR[13] following the published protocol.[53] TcTR concentration was determined by measuring the FAD absorption at 461 nm ($\epsilon_{461\ nm} = 11.3$ mM^{-1} cm^{-1}). 1 unit of TR corresponds to 1 μmol of $T(S)_2$ reduced/min at 25 °C in assay buffer A (20 mM Hepes, pH 7.25 containing 1 mM EDTA and 0.15 M KCl).[11] The enzyme stock solutions used for kinetic determinations were pure as judged from a silver stained SDS−PAGE and had a specific activity of 137 U/mg for TcTR in the $T(S)_2$ reduction assay. Recombinant hGR (E.C. 1.6.4.2) and native hTrxR (E.C. 1.6.4.5) were kindly provided by Prof. Heiner Schirmer and Prof. Katja Becker, Biochemie-Zentrum, Heidelberg.[54,55] Using the DTNB assay, 1 unit of TrxR is defined as the NADPH-dependent production of 2 μmol of 5-thio-2-nitrobenzoate/min ($\epsilon_{412\ nm} = 13.6$ mM^{-1} cm^{-1}). 1 unit of GR activity is defined as the consumption of 1 μmol of NADPH/min ($\epsilon_{340\ nm} = 6.22$ mM^{-1} cm^{-1}). The enzyme stock solutions used for kinetic determinations were pure as judged from a silver-stained SDS−PAGE and had a specific activity of 27 U/mg for hTrxR in the DTNB assay,[56] 200 U/mg for hGR in the GSSG assay, respectively. Recombinant TcLipDH (E.C. 1.8.1.4) was purified from *E. coli* JRG 1342 cells containing the plasmid pQE/*lpd*/-mt gene[14] following a modified preparation described below. The specific activity in the forward reaction was 490 U/mg which corresponds to that of the authentic protein when taking into account that the activity in the forward reaction is about 1.6 times higher than in the reverse reaction.[12,14] Cytochrome *c* and SOD (E.C. 1.15.1.1) were purchased from Sigma. Pig heart LipDH (E.C. 1.8.1.4) was obtained from Boehringer Mannheim. Q-Sepharose was purchased from Pharmacia. Blue Sepharose is a Cibacrom blue 3GA-Sepharose 4B prepared as described.[57] All other reagents were of the highest available purity and were purchased from Biomol, Boehringer, and Sigma. $T(S)_2$ was purchased from Bachem, Switzerland. DL-α-Dihydrolipoamide was prepared by reduction of DL-lipoamide with NaBH$_4$. The procedure employed is a modification of that described by Reed et al.[58] Using 10 mL of 1 M HCl in the acidification step yields crystalline dihydrolipoamide directly.[14] Stock solutions of 40 mM lipoamide and 50 mM dihydrolipoamide were prepared in ethanol and stored at $-$80 °C.

TcTR, hTrxR, and hGR Inhibition Studies. 1. Trypanothione Disulfide Reductase Assay. The standard assay mixture contained 250 μM NADPH and 57 μM $T(S)_2$. IC$_{50}$ values were evaluated in duplicate in the presence of increasing inhibitor concentrations (0.3−50 μM) and 1% DMSO as final concentration. The reaction was started by adding enzyme (10^{-2} units in 500-μL cuvette). Inhibition constants and the type of inhibition were determined at 22 °C in

duplicate for compounds 3_b (at five different inhibitor concentrations 0, 5, 10, 20, 40 μM) and 20_{4-c} (at five different inhibitor concentrations 0, 0.5, 1.0, 1.5, 2.0 μM) with six different $T(S)_2$ concentrations (20, 40, 60, 100, 150, 200 μM) in the presence of 1% DMSO. The reaction was started by adding enzyme (10^{-2} units in a total volume of 500 μL). When inhibition of $T(S)_2$ reduction by 20_{4-c} was measured as a function of $T(S)_2$ concentration, the data were fitted by using a nonlinear regression analysis software (Kaleidagraph) to the following eq 8 for uncompetitive inhibition:[51]

$$V = \frac{V_{max}[S]}{K_m + [S] \ (1 + [I]/K_i)} \tag{8}$$

2. Quinone Reductase Activity of TcTR and hGR. The ability of TcTR to reduce NQs was assayed by monitoring the substrate-dependent oxidation of NADPH at 340 nm ($\epsilon_{340\ nm}$ = 6.22 mM^{-1} cm^{-1}). The assays, in a total volume of 120 μL, contained 0.02 M Hepes, 1 mM EDTA, 0.15 M KCl, pH 7.25 at 22 °C, 200 μM NADPH, 0–100 μM NQ and 0.6 unit TR. The NQs were dissolved in DMSO and the NADPH-oxidase activity was measured at five different concentrations in the presence of 1% DMSO. For the determination of K_m and V_{max} values, the steady-state rates were graphically fitted by using a nonlinear regression analysis software (Kaleidagraph) to the Michaelis–Menten equation,[51] and the turnover number k_{cat} and the dynamic specificity k_{cat}/K_m were calculated. The initial rate for intrinsic NADPH oxidase activity of TcTR has not been subtracted from the rates measured in the presence of NQ, since it proved negligible in comparison to the activity with the bis(NQ). The amount of one-electron reduction of the NQs by TR was monitored at 550 nm by coupling semiquinone formation to the reduction of 25 μM cytochrome c ($\epsilon_{550,cyt\ c(Fe^{2+})}$ = 18.91 mM^{-1} cm^{-1}). Inhibition of the reaction by SOD (0.6 unit in 120-μL cuvette) is a measure of superoxide anion radical generation. The rate of cytochrome c reduction was followed at 550 nm: in the absence of NQ without SOD (NQ$^-$SOD$^-$) and with SOD (NQ$^-$SOD$^+$), in the presence of NQ without SOD (NQ$^+$SOD$^-$) and with SOD (NQ$^+$SOD$^+$). As TR reduces cytochrome c directly,[11] the NQ-dependent cytochrome c reductase activity of TcTR was calculated by subtracting the rate of cytochrome c reduction in the absence of NQ (NQ$^-$SOD$^-$) from the rate of cytochrome c reduction in the presence of NQ (NQ$^+$SOD$^-$). Addition of SOD allowed to calculate the NQ$^{-\bullet}$-dependent cytochrome c reductase of TcTR by subtracting the rate of cytochrome c reduction in the absence of NQ (NQ$^-$SOD$^+$) from the rate of cytochrome c reduction in the presence of NQ (NQ$^+$SOD$^+$). Eq 9 gives the contribution of superoxide anion radicals in the NQ-dependent cytochrome c reductase of TcTR:

$$100\% - \frac{[100(NQ^+SOD^+) - (NQ^-SOD^+)]}{(NQ^+SOD^-) - (NQ^-SOD^-)} \tag{9}$$

At the low-enzyme and high-cytochrome c concentrations (25 μM) used in these experiments, the percentage of one-electron reduction is calculated by dividing the rate of cytochrome c reduction by twice the rate of NADPH oxidation in the presence of 12.5 μM NQ.[17] The amount of one-electron reduction of the NQs by hGR was monitored at 550 nm under the conditions described above for TR.

3. hTrxR Inhibition Studies. The most potent TcTR inhibitors were studied as inhibitors of human TrxR by using the standard assay protocol developed in microtiter plates for inhibitor screening.[39] All reactions with hTrxR were performed in assay buffer C (100 mM sodium phosphate, 2 mM EDTA, pH 7.0). The components for the TrxR assay were added into each well at the following final concentration: 25 μM inhibitor, 200 μM disulfide DTNBA, 500 μM NADPH, 2% DMSO. The reaction was started by adding 80 μL of an enzyme solution containing 8 × 10^{-4} units of native hTrxR. Positive and negative controls were conducted in duplicate with the following components: substrate (final concentration 2% DMSO) with and without enzyme, substrate in the presence of enzyme,

and 25 μM 2,6-dichloroindophenol as reference inhibitor containing 2% DMSO.

4. hGR Inhibition Studies. The effect of the 1,4-NQ upon hGR was studied in the standard assay[59,60] developed for microtiter plates, with the following slight modifications. All enzymic and nonenzymic reactions were conducted in flat-bottomed 96-well microtiter plates (Nunc Inc.) in a total volume of 100 μL. The reactions were allowed to proceed for 20 min at room temperature (22–25 °C) and stopped by addition of acetonitrile and DTNB. The plates were then read using a 405-nm filter in the multiskan microplate reader, as described above. All reactions with hGR were performed in assay buffer C (100 mM sodium phosphate, 2 mM EDTA, pH 7.0). The components for the TrxR assay were added into each well at the following final concentrations: 25 μM inhibitor, 200 μM GSSG, 500 μM NADPH, 1% DMSO. The reaction was started by adding 80 μL of an enzyme solution containing 8 × 10^{-3} units native hGR. Positive and negative controls were made in duplicate by incubating the following components: substrate solution (final concentration 2% DMSO) with and without enzyme, substrate solution in the presence of enzyme, and the reference inhibitor (25 μM isoalloxazine $3b$[28] (10-(3′,5′-dichlorophenyl)-3-methylisoalloxazine), 2% DMSO).

Molecular Modeling. The protein structures were studied on a Silicon Graphics work station using the Insight II module of the MSI software. The CAST program was used for a comparative analysis of the corresponding sites at the dimer interface of TcTR and hGR.[61] This program identifies cavities, pockets, and corresponding channel openings in protein structures. It provides also a measure of area, volume, and circumference of each site and opening. The three-dimensional structures of hGR and TcTR used were those of uncomplexed enzymes accessible at the Protein Data Bank under 3grs[25] and 1aog,[41] respectively, in which the TcTR structure is deposited as a dimer, while for hGR crystallographic symmetry operations were applied to the monomer in order to obtain the homodimer.

TcLipDH and Pig Heart LipDH Inhibition Studies. 1. Purification of Recombinant TcLipDH. *T. cruzi* LipDH was purified from *E. coli* JRG 1342 cells containing the plasmid pQE/lpd/-mt[14] by a modified preparation scheme since the purification scheme based on affinity chromatography on AMP-Sepharose[14] yielded an enzyme species with a relatively low specific activity when compared with the protein isolated from *T. cruzi* epimastigotes.[12] In the procedure described here, the AMP-Sepharose column was replaced by Q-Sepharose and Blue Sepharose columns. The parasite enzyme was isolated in an overall yield of 73% (Table 6) and the protein sample proved to be much more stable during storage. Starting from 2.2 L of bacterial culture, the cell extract was prepared as described.[14] The protein was precipitated by 42–70% ammonium sulfate, centrifuged, and the pellet was dissolved in buffer A (5 mM potassium phosphate, 1 mM EDTA, pH 7.5) yielding fraction I. Following dialysis against buffer B (10 mM potassium phosphate, 1 mM EDTA, pH 7.5) fraction I was centrifuged and applied to a 50-mL Q-Sepharose column equilibrated in buffer B. The column was washed with 150 mL of buffer B at a flow rate of 0.7 mL/min and TcLipDH was eluted by 80 mM KCl in buffer B. Active fractions were pooled and the protein was concentrated and washed with buffer C (5 mM potassium phosphate, 1 mM EDTA, pH 7.0) in a Centriprep 30 concentrator to give fraction II. Fraction II was applied to an 8-mL Blue Sepharose column equilibrated in buffer C at a flow rate of 0.8 mL/min. The column was washed with 25 mL of buffer C, then with 25 mL of buffer D (20 mM potassium phosphate, 1 mM EDTA, 1 mM dithiothreitol, pH 7.0) at a flow rate of 0.6 mL/min. TcLipDH was eluted with buffer E (100 mM potassium phosphate, 100 mM KCl, 1 mM EDTA, 1 mM dithiothreitol, pH 7.0). Active fractions were pooled (fraction III) and concentrated by centrifugation in a Centricon 30 concentrator. 50% Glycerol was added and the pure protein was stored at −20 °C.

2. LipDH Assay. LipDH activity was measured in the forward reaction at 25 °C at 1 mM NAD$^+$ and 1.4 mM

Table 6. Purification of 5.2 mg of TcLipDH from 2.2 L of Recombinant *E. coli* JRG1342 Cells[a]

purification step	resulting fraction	total protein (mg)	total enzyme activity (U)	specific activity (U/mg)	overall yield (%)
extraction	I	4900	4800	1.0	100
42−70% (NH₄)₂SO₄ precipitation, dissolved pellet	II	2500	4530	1.8	94
dialysis	III	1800	4450	2.5	93
ion-exchange chromatography on Q-Sepharose	IV	46	3970	86	83
affinity chromatography on Blue Sepharose, concentration in an Amicon 30 concentrator	V	7.1	3500	490	73

[a] In crude fractions (I−III) the protein concentration was estimated by absorption measurements at 280 nm assuming that 1 mg/mL protein corresponds to an absorbance of 1.0. The protein concentration of homogeneous TcLipDH (V) was determined at 280 nm with an absorption of 1 corresponding to 1.8 mg/mL.

dihydrolipoamide in 50 mM potassium phosphate, 1 mM EDTA, pH 7.0 (assay buffer) in a total volume of 1 mL.[12] The assay mixture was preincubated in order to obtain a stable baseline and the reaction was started by addition of the enzyme. The absorption increase at 340 nm was monitored.[14] Under these conditions, with about 50 ng/mL LipDH in the assay the oxidase activity of the enzyme (see below) is negligible.

3. Quinone Reductase Activity of LipDHs. The NQ reductase activity of LipDH was followed at 31 °C in a Beckmann DU 65 spectrophotometer using microcuvettes. The assay mixture of total volume of 90 μL contained 100 μM NADH and 10 μM to 1 mM of the respective NQ in assay buffer (50 mM potassium phosphate, 1 mM EDTA, pH 7.0). Several stock solutions were prepared for each NQ. Thus all assays contained 5 μL of DMSO which is important because of a slight inhibition (about 20%) of the enzyme by DMSO. The reaction was started by addition of the enzyme, and the absorption decrease at 340 nm was monitored. The intrinsic oxidase activity of LipDH was measured with 100 μM NADH in the absence of any substrate. The assays contained between 0.1 and 2.5 μg/mL enzyme. The generation of semiquinones was monitored by coupling the reduction of NQs to cytochrome *c* reduction. The assay mixture contained in a total volume 90 μL, 50 mM potassium phosphate, pH 7.0, 100 μM NADH, 50 μM cytochrome *c*, and 50 μM of the respective NQ. The reaction was started by addition of the enzyme and the absorption increase at 550 nm was followed at 31 °C. At pH values < 7.2 reduction of cytochrome *c* by benzohydroquinones should be negligible whereas reduction by the semiquinones is high.[3] Thus the efficiency of one-electron reduction can be calculated by dividing the rate of cytochrome *c* reduction by twice the rate of NADH oxidation.[62] At low enzyme activities and high cytochrome *c* concentrations (30−40 μM) more than 90% of the semiquinone formed is trapped.[3] To distinguish between direct and superoxide-mediated reduction of cytochrome *c* by the semiquinones, 5 μL of SOD (0.6 mg/mL) was added to the assay after 3 min. The K_m and V_{max} values were derived from Lineweaver−Burk plots.

Parasites. *L. donovani* (strain MHOM/ET/67/L82) was maintained routinely in special pathogen-free (SPF) female Golden hamsters (Wright's strain, Charles Rivers Ltd.) by passage every 12 weeks. *T. cruzi* (strain MHOM/BR/OO/Y) trypomastigotes were derived from MDCK fibroblasts in Dulbecco's modified Eagle medium (Life Technologies Ltd., Paisley, Scotland) with 10% heat-inactivated fetal calf serum (HIFCS) (Harlan Sera-Lab., Crawley, U.K.) at 37 °C in an atmosphere of 5% CO₂−air mixture. *T. brucei brucei* (strain S427) bloodstream form trypomastigotes were maintained in HMI-18 medium[63] supplemented with 20% HIFCS at 37 °C in a 5% CO₂−air mixture.

In Vitro Antitrypanosomal Bioassays. *L. donovani* and *T. cruzi*: Peritoneal macrophages were harvested from female CD1 mice (Charles River Ltd., Margate U.K.) by peritoneal lavage 24 h after induction by soluble starch (Merk Ltd., Leics, U.K.). After two washes in medium the exudate cells were dispensed into 16-well Lab-tek tissue culture slides (Nunc Inc., IL) at 4×10^5/mL in a volume of 100 μL of RPMI-1640 medium (Sigma-Aldrich Co. Ltd., Dorset, U.K.) plus 10% HIFCS. After 24 h, macrophages were infected at a ratio of 10:1 (4×10^6/ml, 100 μL/well) with *L. donovani* amastigotes freshly isolated from hamster spleen or at a ratio of 5:1 (2×10^5/well) with *T. cruzi* trypomastigotes derived from the MDCK fibroblast overlay. Infected macrophages were then maintained in the presence of the drug in a 3-fold dilution series, with quadruplicate cultures at each concentration, for 5 days for *L. donovani* cultures and 3 days for *T. cruzi* cultures. After these periods of drug exposure slides were methanol-fixed and Giemsa-stained, and drug activity was determined by counting the percentage of macrophages cleared of amastigotes in treated cultures in comparison with untreated cultures.[64] ED₅₀ values were determined by sigmoidal regression analysis (MS *xl*fit). Sodium stibogluconate (NaSbᵛ) (Glaxo-Wellcome, Dartford, U.K.) and nifurtimox (Bayer, U.K.) were used as the respective control drugs.

***T. brucei brucei*:** Tests were performed in HMI-18 medium as described above.[63] Compounds were tested in triplicate in a 3-fold dilution series from the highest concentration of 30 μM. Parasites were diluted to 2×10^5/mL and added in equal volume to the test compounds in 96-well, flat-bottom Microtest III tissue culture plates (Becton Dickinson and Co., NJ). Appropriate controls with pentamidine isethionate (Rhone-Poulonc-Rorer) as the positive were set up in parallel. Plates were maintained for 3 days at 37 °C in a 5% CO₂−air mixture. The antiparasitic activity of the compounds was determined by use of a tetrazolium salt colorimetric assay[65] on day 3. ED₅₀ values were determined by sigmoidal regression analysis.

Supporting Information Available: Details of chemical procedures and analytical data. This material is available free of charge via the Internet at http://pubs.acs.org.

References

(1) O'Brien, P. J. Molecular mechanisms of quinone cytotoxicity. *Chem. Biol. Interact.* **1991**, *80*, 1−41.

(2) Zuman, P. *Substituent effects in organic polarography*; Plenum Press: New York, 1967.

(3) Iyanagi, T.; Yamazaki, I. One-electron-transfer reactions in biochemical systems (V. Difference in the mechanism of quinone reduction by the NADH dehydrogenase and the NAD(P)H dehydrogenase (DT-diaphorase). *Biochim. Biophys. Acta* **1970**, *216*, 282−294.

(4) Nakamura, M.; Yamazaki, I. One-electron-transfer reactions in biochemical systems. VI. Changes in electron-transfer mechanism of lipoamide dehydrogenase by modification of sulfhyhdyl groups. *Biochim. Biophys.* Acta **1972**, *267*, 249−257.

(5) Croft, S. L.; Evans, A. T.; Neal, R. A. The activity of plumbagin and other electron carriers against *Leihmania donovani* and *Leishmania mexicana amazonensis. Ann. Trop. Med. Parasitol.* **1985**, *79*, 651−653.

(6) Croft, S. L.; Hogg, J.; Gutteridge, W. E.; Hudson, A. T.; Randall, A. W. The activity of hydroxynaphthoquinones against *Leihmania donovani. J. Antimicrob. Chemother.* **1992**, *30*, 827−832.

(7) Boveris, A.; Docampo, R.; Turrens, J. F.; Stoppani, A. O. M. Effect of β-lapachone on superoxide anion and hydrogen peroxide production in *Trypanosoma cruzi. Biochem. J.* **1978**, *175*, 431−439.

(8) Krauth-Siegel, R. L.; Coombs, G. H. Enzymes of parasite thiol metabolism as drug targets. *Parasitol. Today* **1999**, *15*, 404−409.

(9) Faerman, C. H.; Savvides, S. N.; Strickland, C.; Breidenbach, M. A.; Ponasik, J. A.; Ganem, B.; Ripoll, D.; Krauth-Siegel, R. L.; Karplus, P. A. Charge is the major discriminating factor for glutathione reductase versus trypanothione reductase inhibitors. *Bioorg. Med. Chem.* **1996**, *4*, 1247−1253.

(10) Williams, C. H., Jr. In *Chemistry and Biochemistry of Flavoenzymes*; Müller, F., Ed.; CRC Press: Boca Raton, FL, 1992; Vol. III.

(11) Krauth-Siegel, R. L.; Enders, B.; Henderson, G. B.; Fairlamb, A. H.; Schirmer, R. H. Trypanothione reductase from *Trypanosoma cruzi*: purification and characterization of the crystalline enzyme. *Eur. J. Biochem.* **1987**, *164*, 123−128.

(12) Lohrer, H.; Krauth-Siegel, R. L. Purification and characterization of lipoamide dehydrogenase from *Trypanosoma cruzi. Eur. J. Biochem.* **1990**, *194*, 863−869.

(13) Sullivan, F. X.; Walsh, C. T. Cloning, sequencing, overproduction and purification of trypanothione reductase from *Trypanosoma cruzi. Mol. Biochem. Parasitol.* **1991**, *44*, 145−148.

(14) Schöneck, R.; Billaut-Mulot, O.; Numrich, P.; Ouaissi, M. A.; Krauth-Siegel, R. L. Cloning, sequencing and functional expression of dihydrolipoamide dehydrogenase from the human pathogen *Trypanosoma cruzi. Eur. J. Biochem.* **1997**, *243*, 739−747.

(15) Blumenstiel, K.; Schöneck, R.; Yardley, V.; Croft, S. L.; Krauth-Siegel, R. L. Nitrofuran drugs as common subversive substrates of *Trypanosoma cruzi* lipoamide dehydrogenase and trypanothione reductase. *Biochem. Pharmacol.* **1999**, *58*, 1791−1799.

(16) Krauth-Siegel, R. L.; Schöneck, R. Trypanothione reductase and lipoamide dehydrogenase as targets for a structure-based drug design. *FASEB J.* **1995**, *9*, 1138−1146.

(17) Cenas, N. K.; Arscott, D.; Williams, C. H.; Blanchard, J. S. Mechanism of reduction of quinones by *Trypanosoma congolense* trypanothione reductase. *Biochemistry* **1994**, *33*, 2509−2515.

(18) Henderson, G. B.; Ulrich, P.; Fairlamb, A. H.; Rosenberg, I.; Pereira, M.; Sela, M.; Cerami, A. Subversive substrates for the enzyme trypanothione disulfide reductase: alternative approach to chemotherapy of Chagas disease. *Proc. Natl. Acad. Sci. U.S.A.* **1988**, *85*, 5374−5378.

(19) Jockers-Scherübl, M. C.; Schirmer, R. H.; Krauth-Siegel, R. L. Trypanothione reductase from *Trypanosoma cruzi*. Catalytic properties of the enzyme and inhibition studies with trypanocidal compounds. *Eur. J. Biochem.* **1989**, *180*, 267−272.

(20) Schirmer, R. H.; Müller, J. G.; Krauth-Siegel, R. L. Disulfide reductase inhibitors as chemotherapeutic agents: the design of drugs for trypanosomiasis and malaria. *Angew. Chem., Int. Ed. Engl.* **1995**, *34*, 141−154.

(21) Bironaite, D.; Cenas, N. K.; Kulys, J. J. The inhibition of glutathione reductase by quinones. *Z. Naturforsch. C* **1991**, *46*, 966−968.

(22) Lüöng, R. M.; McKie, J. H.; Douglas, K. T.; Dascombe, M. J.; Vale, J. Inhibitors of glutathione reductase as potential antimalarial drugs. Kinetic cooperativity and effect of dimethyl sulphoxide on inhibition kinetics. *J. Enzymol. Inhib.* **1998**, *13*, 327−345.

(23) Cenas, N. K.; Rakauskiené, G. A.; Kulys, J. J. One- and two-electron reduction of quinones by glutathione reductase. *Biochim. Biophys. Acta* **1989**, *973*, 399−404.

(24) Bironaite, D. A.; Anusevicius, Z.; Jacquot, J.-P.; Cenas, N. K. Interaction of quinones with *Arabidopsis thaliana* thioredoxin reductase. *Biochim. Biophys. Acta* **1998**, *1383*, 82−92.

(25) Karplus, P. A.; Schulz, G. E. Refined Structure of glutathione reductase at 1.54 Å Resolution. *J. Mol. Biol.* **1987**, *195*, 701−729.

(26) Karplus, P. A.; Pai, E. F.; Schulz, G. E. A crystallographic study of the glutathione binding site of glutathione reductase at 0.3-nm resolution. *Eur. J. Biochem.* **1989**, *178*, 693−703.

(27) Savvides, S.; Karplus, P. A. Kinetics and crystallographic analysis of human glutathione reductase in complex with a xanthene inhibitor. *J. Biol. Chem.* **1996**, *271*, 8101−8107.

(28) Schönleben-Janas, A.; Kirsch, P.; Mittl, P. R. E.; Schirmer, R. H.; Krauth-Siegel, L. Inhibition of human glutathione reductase by 10-arylisoalloxazines: crystallographic, kinetic, and electrochemical studies. *J. Med. Chem.* **1996**, *39*, 1549−1554.

(29) Krauth-Siegel, R. L.; Arscott, L. D.; Schönleben-Janas, A.; Schirmer, R. H.; Williams, C. H. Role of active site tyrosine residues in catalysis by human glutathione reductase. *Biochemistry* **1998**, *37*, 13968−13977.

(30) Kallmayer, H. J. Synthese und Eigenschaften alkylierter Aminonaphthochinone. *Arch. Pharmaz.* **1974**, *37*, 806−814.

(31) Ohta, S.; Hinata, Y.; Yamashita, M.; Kawasaki, I.; Jinda, Y.; Horie, S. One-step synthesis of 1,2,3,4-Tetrahydrobenzo[*g*]-quinazoline-5,10-dione derivatives from vitamin *K*₃. *Chem. Pharm. Bull.* **1994**, *42*, 1730−1735.

(32) Ohta, S.; Hinata, Y.; Kawasaki, I.; Yamashita, M. Photooxidation of 2-Methylamino-3-(1-piperidinylmethyl)-1,4-naphthoquinone. *Chem. Pharm. Bull.* **1994**, *42*, 2360−2362.

(33) Couladouros, E. A.; Plyta, Z. F.; Papageorgiou, V. P. A general procedure for the efficient synthesis of (alkylamino)naphthoquinones. *J. Org. Chem.* **1996**, *61*, 3031−3033.

(34) Ohta, S.; Hinata, Y.; Yamashita, M.; Kawasaki, I.; Shoji, T.; Yoshikawa, H.; Obana, Y. Synthetic approaches to 3-Amino-1,4-naphthoquinone-2-carboxylic acid derivatives and photochemical synthesis of novel 1,4,5,10-Tetrahydro-5,10-dioxo-2*H*-naphth[2,3-*d*][1,3]oxazine derivatives. *Chem. Pharm. Bull.* **1994**, *42*, 1185−1190.

(35) Salmon-Chemin, L.; Lemaire, A.; De Freitas, S.; Deprez, B.; Sergheraert, C.; Davioud-Charvet, E. Parallel synthesis of a library of 1,4-naphthoquinones and automated screening of potential inhibitors of trypanothione reductase from *Trypanosoma cruzi. Bioorg. Med. Chem. Lett.* **2000**, *10*, 631−635.

(36) Anderson, J. M.; Kochi, J. K. Silver(I)-catalyzed oxidative decarboxylation of acids by peroxydisulfate. The role of silver-(II). *J. Am. Chem. Soc.* **1970**, *92*, 1651−1659.

(37) Cenas, N.; Bironaite, D.; Dickancaite, E.; Anusevicius, Z.; Sarlauska, J.; Blanchard, J. S. Chinifur, a selective inhibitor and "subversive substrate" for *Trypanosoma congolense* trypanothione reductase. *Biochem. Biophys. Res. Commun.* **1994**, *204*, 224−229.

(38) Henderson, P. J. F. Statistical analysis of enzyme kinetic data. In *Enzyme assays: a practical approach*; Eisenthal, R., Danson, M. J., Eds.; 1995.

(39) Davioud-Charvet, E.; Becker, K.; Landry, V.; Gromer, S.; Logé, C.; Sergheraert, C. Synthesis of alternative substrates for trypanothione reductase and thioredoxin reductase: an inexpensive microtiter colorimetric assay for inhibitor screening. *Anal. Biochem.* **1999**, *268*, 1−8.

(40) Jacoby, E. M.; Schlichting, I.; Lantwin, C. B.; Kabsch, W.; and Krauth-Siegel, R. L. Crystal structure of the *Trypanosoma cruzi* trypanothione reductase-mepacrine complex. *Proteins* **1996**, *24*, 73−80.

(41) Zhang, Y.; Bond, C. S.; Bailey, S.; Cunningham, M. L.; Fairlamb, A. H.; Hunter, W. N. The crystal structure of trypanothione reductase from the human pathogen *Trypanosoma cruzi* at 2.3 Å resolution. *Protein Sci.* **1996**, *5*, 52−61.

(42) Misaka, E.; Kawahara, Y.; Nakanishi, K. Studies on menadione reductase in yeast. III The identity of menadione reductase with lipoamide dehydrogenase. *J. Biochem.* **1965**, *58*, 436−443.

(43) Bergeron, R. J.; Feng, Y.; Weimar, W. R.; McManis, J. S.; Dimova, H.; Porter, C.; Raisler, B.; Phanstiel, O. A comparison of structure−activity relationships between spermidine and spermine analogue antineoplastics. *J. Med. Chem.* **1997**, *40*, 1475−1494.

(44) Bonnet, B.; Soullez, D.; Girault, S.; Maes, L.; Landry, V.; Davioud-Charvet, E.; Sergheraert, C. Trypanothione reductase inhibition/trypanocidal activity relationships in a 1,4-bis(3-aminopropyl)piperazine series. *Biorg. Med. Chem.* **2000**, *8*, 95−103.

(45) Girault, S.; Baillet, S.; Horvath, D.; Lucas, V.; Davioud-Charvet, E.; Tartar, A.; Sergheraert, C. New potent inhibitors of trypanothione reductase from *Trypanosoma cruzi* in the 2-aminodiphenylsulfides series. *Eur. J. Med. Chem.* **1997**, *32*, 39−52.

(46) Bonnet, B.; Soullez, D.; Davioud-Charvet, E.; Landry, V.; Horvath, D.; Sergheraert, C. New spermine and spermidine derivatives as potent inhibitors of *Trypanosoma cruzi* trypanothione reductase. *Bioorg. Med. Chem.* **1997**, *5*, 1249−1256.

(47) Ponasik, J. A.; Strickland, C.; Faerman, C.; Savvides, S., Karplus, P. A.; Ganem, B. Kukoamine A and other hydrophobic acylpolyamines: potent and selective inhibitors of *Crithidia fasciculata* trypanothione reductase. *Biochem. J.* **1995**, *311*, 371−375.

(48) Bonse, S.; Krauth-Siegel, R. L. Irreversible inhibitors of *T. cruzi* trypanothione reductase: kinetic and crystallographic studies. In *Flavins and Flavoproteins*; Rudolf Weber Agency for Scientific Publication: Berlin, 1999.

(49) Gallwitz, H.; Bonse, S.; Martinez-Cruz, A.; Schlichting, I.; Schumacher, K.; Krauth-Siegel, R. L. Ajoene is an inhibitor and subversive substrate of human glutathione reductase and *Trypanosoma cruzi* trypanothione reductase: crystallographic, kinetic, and spectroscopic studies. *J. Med. Chem.* **1999**, *42*, 364−372.

(50) Leichus, B. N.; Bradley, M.; Nadeau, K.; Walsh, C. T.; Blanchard, J. S. Kinetic Isotope effect analysis of the reaction catalyzed by *Trypanosoma congolense* trypanothione reductase. *Biochemistry* **1992**, *31*, 6414−6420.

(51) Segel, I. H. *Enzyme Kinetics*; Wiley: London, 1975.

(52) Bonse, S.; Santelli-Rouvier, C.; Barbe, J.; Krauth-Siegel, R. L. Inhibition of *Trypanosoma cruzi* trypanothione reductase by acridines: kinetic studies and structure−activity relationships. *J. Med. Chem.* **1999**, *42*, 5448−5454.

(53) Krauth-Siegel, R. L.; Sticherling, C.; Jöst, I.; Walsh, C. T., Pai, E. F.; Kabsch, W., Lantwin, C. B. Crystallization and preliminary crystallographic analysis of trypanothione reductase from *Trypanosoma cruzi*, the causative agent of Chagas' disease. *FEBS Lett.* **1993**, *317*, 105−108.

(54) Nordhoff, A.; Bücheler, U. S.; Werner, D.; Schirmer, R. H. Folding of the four domains and dimerization are impaired by Gly446→Glu exchange in human glutathione reductase. Implications for the design of antiparasitic drugs. *Biochemistry* **1993**, *29*, 4022−4030.

(55) Gromer, S.; Arscott, L. D.; Williams, C. H.; Schirmer, R. H.; Becker, K. Human placenta thioredoxin reductase. *J. Biol. Chem.* **1998**, *273*, 20096−20101.

(56) Holmgren, A.; Björnstedt, M. Thioredoxin and thioredoxin reductase. *Methods Enzymol.* **1995**, *252*, 199−208.

(57) Dean, P. D.; Watson, D. H. Protein purification using immobilized triazine dyes. *J. Chromatogr.* **1979**, *165*, 301−319.

(58) Reed, J. W.; Koike, M.; Levitch, M. E.; Leach, F. R. Studies on the nature and reactions of protein-bound lipoic acid. *J. Biol. Chem.* **1958**, *232*, 143−158.

(59) Baker, M. A.; Cerniglia, G. J.; Zaman, A. Microtiter plate assay for the measurement of glutathione and glutathione disulfide in large numbers of biological samples. *Anal. Biochem.* **1990**, *190*, 360−365.

(60) Clarke, J. B.; Fortes, M. A.; Giovanni, A.; Brewster, D. W. Modification of an enzymatic glutathione assay for the microtiter plate and the determination of glutathione in rat primary cortical cells. *Toxicol. Methods* **1996**, *6*, 223−230.

(61) Liang, J.; Edelsbrunner, H.; Woodward, C. Anatomy of protein pockets and cavities: measurement of binding site geometry and implications for ligand design. *Protein Sci.* **1998**, *7*, 1884−1897.

(62) Vienozinskis, J.; Butkus, A.; Cenas, N.; Kulys, J. The mechanism of the quinone reductase reaction of pig heart lipoamide dehydrogenase. *Biochem. J.* **1990**, *269*, 101−105.

(63) Hirumi, H.; Hirumi, K. Continuous cultivation of *Trypanosoma brucei* blood stream forms in a medium containing a low concentration of serum protein without feeder cell layers. *J. Parasitol.* **1989**, *75*, 985−989.

(64) Neal, R. A.; Croft, S. L. An in vitro system for determining the activity of compounds against the intracellular amastigote form of *Leishmania donovani*. *J. Antimicrobiol. Chemother.* **1984**, *14*, 312−317.

(65) Ellis, J. A.; Fish, W. R.; Sileghem, M.; McOdimba F. A colorimetric assay for trypanosome viability and metabolic function. *Vet. Parasitol.* **1993**, *50*, 143−149.

(66) Hubbard S. J.; Thornton J. M. NACCESS Computer Program; Department of Biochemistry and Molecular Biology, University College London.